



**US Army Corps  
of Engineers®**  
Engineer Research and  
Development Center

## **A Reconnaissance Snow Survey Across Northwest Territories and Nunavut, Canada, April 2007**

Matthew Sturm, Chris Derksen, Glen Liston, Arvids Silis,  
Daniel Solie, Jon Holmgren, and Henry Huntington

February 2008

# **A Reconnaissance Snow Survey Across Northwest Territories and Nunavut, Canada, April 2007**

Matthew Sturm and Jon Holmgren

*Cold Regions Research and Engineering Laboratory  
U.S. Army Engineer Research and Development Center  
Fort Wainwright, Alaska*

Chris Derksen and Arvids Silis

*Climate Research Division  
Environment Canada  
Toronto, Ontario*

Glen Liston

*Cooperative Institute for Research and Engineering in the Atmosphere  
Colorado State University  
Fort Collins, Colorado*

Daniel Solie

*University of Alaska Fairbanks  
Fairbanks, Alaska*

Henry Huntington

*Huntington Consulting  
Anchorage, Alaska*

Approved for public release; distribution is unlimited.

**Abstract:** During April 2007, a coordinated series of snow measurements were made across the Northwest Territories and Nunavut, Canada, during a 4200-km snowmobile traverse from Fairbanks, Alaska, to Baker Lake, Nunavut. While detailed, local snow measurements have been made as part of ongoing studies at tundra field sites in this region (Daring Lake and Trail Valley Creek in the Northwest Territories), systematic measurements at the regional scale have not been previously collected across this region. Consistent with observations of tundra snow in Alaska and northern Manitoba, the snow cover consisted of depth hoar and wind slab with small and ephemeral fractions of new, recent, and icy snow. The snow was shallow (<40 cm deep), usually with less than six layers. Where deposited on lake and river ice, the snow was shallower, denser, and more metamorphosed than where deposited on tundra. The snow characteristics were highly variable at a local scale, but no longitudinal gradients in snow distribution, magnitude, or structure were detected. Lakes and lake ice confounded passive microwave remote sensing of the snow cover in this area because the lake signal overwhelmed the snow signal. Consequently, challenges remain in developing methods to monitor this snow cover by satellite.

**DISCLAIMER:** The contents of this report are not to be used for advertising, publication, or promotional purposes. Citation of trade names does not constitute an official endorsement or approval of the use of such commercial products. All product names and trademarks cited are the property of their respective owners. The findings of this report are not to be construed as an official Department of the Army position unless so designated by other authorized documents.

**DESTROY THIS REPORT WHEN NO LONGER NEEDED. DO NOT RETURN IT TO THE ORIGINATOR.**

# Contents

<b>Preface</b> .....	<b>vi</b>
<b>1 Introduction</b> .....	<b>1</b>
<b>2 Study Area</b> .....	<b>2</b>
<b>3 Measurements</b> .....	<b>5</b>
<b>4 Results</b> .....	<b>6</b>
General Nature of the Snowpack .....	6
Distributions of Depth, Density, and SWE.....	7
Stratigraphy .....	13
Density and SWE .....	22
SWE to Depth Relationship.....	22
Fixed Transect vs. Roving Transects.....	24
Longitudinal Gradients.....	27
The Nature of the North American Tundra Snow Cover .....	30
Passive Microwave Implications .....	31
<b>5 Discussion</b> .....	<b>47</b>
<b>6 Conclusion</b> .....	<b>49</b>
<b>References</b> .....	<b>50</b>
<b>Appendix A: NIR Images</b> .....	<b>53</b>
<b>Appendix B: Snow Depths</b> .....	<b>59</b>
<b>Appendix C: Soot Measurements</b> .....	<b>70</b>
<b>Appendix D: Mercury Measurements</b> .....	<b>72</b>
<b>Appendix E: Ion Measurements</b> .....	<b>75</b>
<b>Appendix F: Isotope Measurements</b> .....	<b>78</b>
<b>Report Documentation Page</b> .....	<b>81</b>

## Figures and Tables

### Figures

Figure 1. Map of the SnowSTAR-2007 traverse .....	2
Figure 2. Snow stratigraphy at site KD-7 (Yamba Lake) .....	7
Figure 3. Typical snow depth profiles for lake and tundra sites .....	8
Figure 4. PDFs of measured snow depth .....	9
Figure 5. PDFs of measured bulk density .....	10
Figure 6. PDFs of measured SWE .....	11
Figure 7. PDFs of measured snow depths from previous traverses .....	13
Figure 8. Firnspiegel produced by the April 6 <sup>th</sup> rain-on-snow event .....	15
Figure 9. NIR snow stratigraphy photographs for a pair of adjacent lake and tundra sites .....	18
Figure 10. Relative abundance of snow types by layer .....	20
Figure 11. Comparison of mean pit density with snow core density .....	22
Figure 12. SWE versus depth .....	23
Figure 13. Relationships between fixed and roving transect snow depths .....	25
Figure 14. Relationships between fixed and roving transect SWE .....	26
Figure 15. Sites used for analysis of longitudinal gradients .....	27
Figure 16. Longitudinal gradients in depth, density, and SWE for terrestrial and lake measurements .....	29
Figure 17. Vertically polarized AMSR-E brightness temperatures for April 17 .....	34
Figure 18. AMSR-E brightness temperature time series for lake-rich and lake-poor grid cells .....	37
Figure 19. AMSR-E 36.5-GHz polarization gradient for April 3 versus April 9 .....	38
Figure 20. Relationships between snow depth and ice thickness .....	39
Figure 21. Vertically polarized AMSR-E brightness temperatures for April 3 .....	41
Figure 22. AMSR-E brightness temperature time series for the Great Bear Lake surface measurement sites .....	45

**Tables**

Table 1. Sites where snow measurements were made.....	3
Table 2. Summary of measured depth, density, and SWE probability distribution functions .....	9
Table 3. Overview of snow grain classification used during the traverse .....	14
Table 4. Stratigraphy statistics .....	15
Table 5. Summary of snowpack stratigraphic composition by site .....	16
Table 6. Grain sizes by snow texture type .....	21
Table 7. Grain size by snowpit substrate .....	21
Table 8. Correlation results for snow parameters versus longitude .....	28
Table 9. Comparison of SnowSTAR 2007 data with previous campaigns .....	31
Table 10. Summary of measurements across Great Bear Lake .....	39
Table 11. AMSR-E Brightness temperature ranges for the Great Bear Lake region .....	43
Table 12. Regression results for coincident AMSR-E brightness temperatures and surface measurements of snow depth and ice thickness .....	44

## **Preface**

This report was prepared by Matthew Sturm, Terrestrial and Cryospheric Sciences Branch (TCSB), Cold Regions Research and Engineering Laboratory (CRREL), U.S. Army Engineer Research and Development Center (ERDC), Hanover, NH; Chris Derksen, Climate Research Division, Environment Canada, Toronto, Ontario; Glen Liston, Cooperative Institute for Research and Engineering in the Atmosphere, Colorado State University, Fort Collins, CO; Arvids Silis, Climate Research Division, Environment Canada, Toronto, Ontario; Daniel Solie, University of Alaska Fairbanks, Fairbanks, AK; Jon Holmgren, TCSB, CRREL/ERDC; and Henry Huntington, Huntington Consulting, Anchorage, AK.

The work described here was supported by National Science Foundation Grants ARC-0700233 and 0632131. The participation of the Canadian members of the team was supported by funds provided by Environment Canada. The authors thank Dr. Robert Davis, Director of CRREL, for his support of the project, Dave Andersen for maintaining the website that they operated during the expedition, the Arctic Research Consortium of the United States for hosting the website, and all of the fine people they met along the way who helped them welcomed them, and ensured that their trip was a success.

The report was prepared under the general supervision of Janet Hardy, Chief, TCSB; Dr. Justin Berman, Chief, Research and Engineering Division; and Dr. Robert E. Davis, Director, CRREL.

The Commander and Executive Director of ERDC is COL Richard B. Jenkins. The Director is Dr. James R. Houston.

# 1 Introduction

During April 2007, we made a coordinated series of snow measurements across the Northwest Territories (NWT) and Nunavut, Canada. These were made while traversing by snowmobile from Fairbanks, Alaska, to Baker Lake, Nunavut, as part of the SnowSTAR-2007 expedition. The purpose of the measurements was to document the general nature of the snowpack across this region. Detailed, local snow measurements have been made as part of on-going studies at a few places along the traverse route like Daring Lake and Trail Valley Creek in the Northwest Territories, but to our knowledge, systematic measurements at the regional scale have not been collected in this area before.



## 2 Study Area

The study area and the route of SnowSTAR-2007 are shown in Figure 1. Measurements were made at the 45 locations listed in Table 1. The route included a) long stretches on frozen lakes, including Great Bear Lake, the seventh largest lake in the world, b) areas of rolling tundra, and c) areas of rocky, morainal tundra. A more detailed description of the exploration history and physiography of the region can be found in Tyrrell (1897) and Douglas (1914).

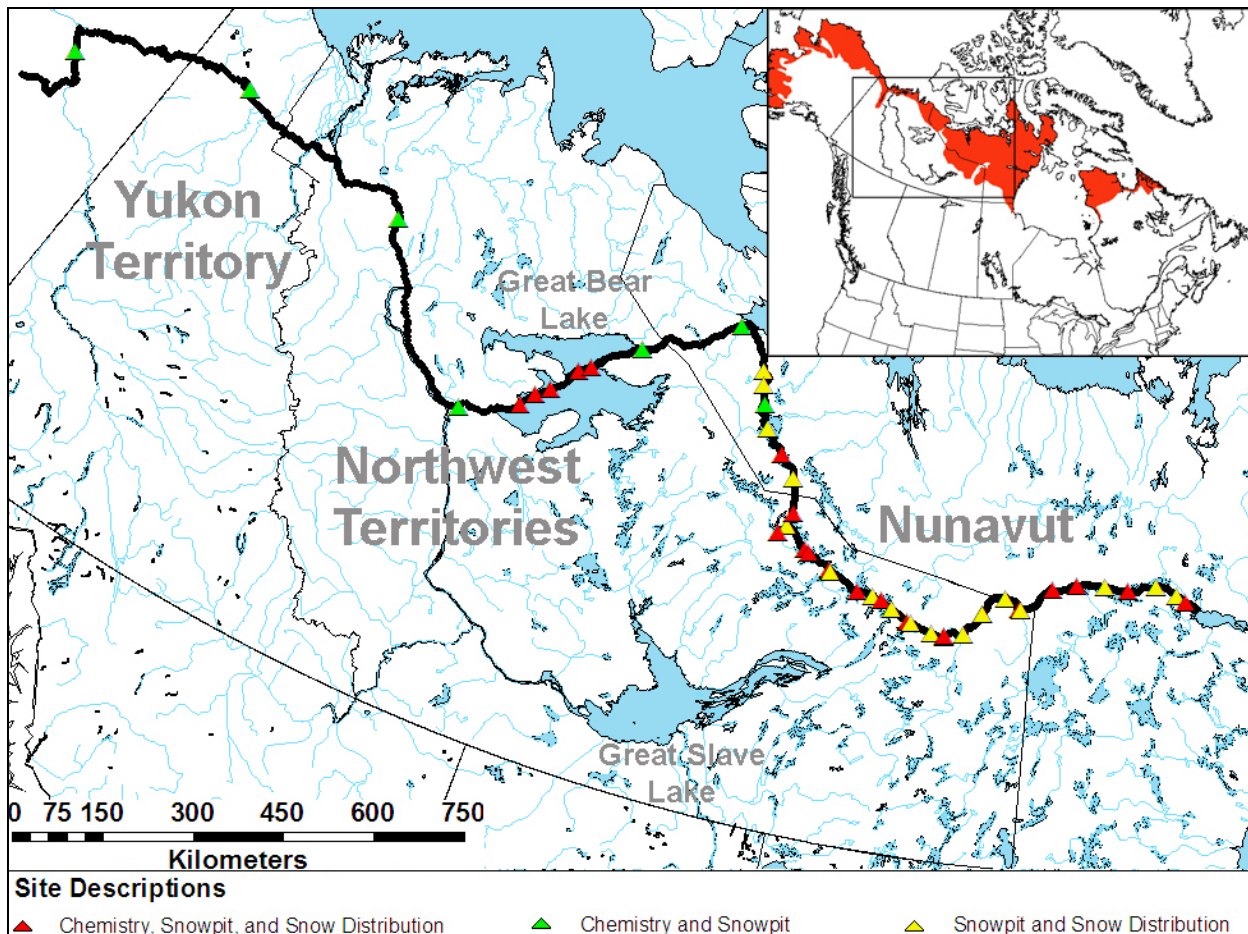


Figure 1. Map of the SnowSTAR-2007 traverse, which started in Fairbanks, Alaska, entered Canada in the Yukon Territory, crossed the Northwest Territories, and ended in Nunavut. Sites where snow measurements were made are denoted by triangles. The approximate extent of tundra snow across continental North America is highlighted in red in the map inset.

Table 1. Sites where snow measurements were made.

Site Name	Description	Date	Latitude	Longitude	Chemistry	Snowpit	Depth	SWE	Ice Thickness	NIR photos
Yukon River	River	19-Mar-07	66.25552	144.76890	√	√				√
Porcupine River	River	25-Mar-07	67.56833	138.28667	√	√				√
MacKenzie River	River	30-Mar-07	67.16000	130.25667	√	√				√
Small lake near Deline	Lake	01-Apr-07	64.93390	124.77438	√	√				√
Great Bear 1 (GB1)	Lake	02-Apr-07	65.37922	122.66280	√	√	√	√	√	√
Great Bear 2 (GB2)	Lake	03-Apr-07	65.60676	122.26140	√	√	√	√	√	√
Great Bear 3 (GB3)	Lake	03-Apr-07	65.78752	121.78390	√	√	√	√	√	√
Great Bear 4 (GB4)	Lake	04-Apr-07	66.22479	121.06220	√	√	√	√	√	√
Great Bear 5 (GB5)	Lake	04-Apr-07	66.35284	120.63710	√	√	√	√	√	√
Dease River	River	06-Apr-07	66.90020	118.93787	√	√				√
Bloody Falls	Tundra	10-Apr-07	67.74865	115.37532	√	√				√
KD1	Tundra	11-Apr-07	67.17657	113.98170		√	√			√
KD2	Lake	11-Apr-07	66.95060	113.82645		√	√			√
KD3	Lake	11-Apr-07	66.65447	113.55992	√	√	√			√
KD4	Lake	11-Apr-07	66.29432	113.23383		√	√			√
Rockinghorse Lake	Lake	12-Apr-07	65.95683	112.42167	√	√	√			√
KD6	Tundra	12-Apr-07	65.62297	111.73620		√	√			√
Yamba Lake	Lake	13-Apr-07	65.08667	111.45447	√	√	√	√	√	√
Lake Providence	Tundra	15-Apr-07	64.74738	111.85403	√	√	√	√		√
Diavik (DB1)	Tundra	17-Apr-07	64.58344	110.75402	√	√	√	√		√
Lac de Gras (DB2)	Lake	17-Apr-07	64.52760	110.53655	√	√	√	√	√	√
Thonokied Lake (DB3)	Lake	18-Apr-07	64.35160	109.68070	√	√	√	√	√	√
Thonokied (DB4)	Tundra	18-Apr-07	64.31560	109.62797		√	√	√		√
Aylmer Lake (DB5)	Lake	18-Apr-07	64.08630	108.50971	√	√	√	√	√	√
Aylmer/Clinton-Colden	Tundra	19-Apr-07	64.04894	107.90361		√	√	√		√
Clinton-Colden Lake (DB7)	Lake	19-Apr-07	64.01122	107.57671	√	√	√	√	√	√
Clinton-Colden	Tundra	19-Apr-07	63.90762	107.17368		√	√	√		√
Sifton Lake (DB9)	Lake	20-Apr-07	63.75079	106.54487	√	√	√	√	√	√
North Hanbury	Tundra	20-Apr-07	63.73479	106.40660		√	√	√		√
West Hoare	Tundra	20-Apr-07	63.61753	105.58390		√	√	√		√
Hoare Cabin (DB12)	Tundra	21-Apr-07	63.59357	105.14859		√	√	√		√
Hoare Lake (DB13)	Lake	21-Apr-07	63.61069	105.12755	√	√	√	√	√	√
Hanbury/Thelon (DB14)	Tundra	21-Apr-07	63.67893	104.44458		√	√	√		√
Hornby Point (DB16)	Forest	22-Apr-07	64.03854	103.85468	√	√	√	√		√

Table 1 (cont.). Sites where snow measurements were made.

Hornby Thelon (DB15)	River	22-Apr-07	64.04111	103.84445		√	√	√		√
Thelon Nunavut (DB17)	River	22-Apr-07	64.32897	103.10192		√	√	√		√
Thelon Lookout Point	River	23-Apr-07	64.17569	102.50803	√	√	√	√		√
Lookout Point (DB19)	Tundra	23-Apr-07	64.16911	102.49567		√	√	√		√
Thelon Cabin (DB20)	Tundra	23-Apr-07	64.53258	101.35525	√	√	√	√		√
Beverly Lake (DB21)	Lake	24-Apr-07	64.62036	100.47297	√	√	√	√	√	√
Aberdeen (DB22)	Tundra	24-Apr-07	64.62642	99.44250		√	√	√		√
Aberdeen Lake (DB23)	Lake	25-Apr-07	64.57758	98.54950	√	√	√	√	√	√
South Schultz (DB24)	Tundra	25-Apr-07	64.66439	97.50247		√	√	√		√
North Baker (DB25)	Tundra	26-Apr-07	64.52308	96.75625		√	√	√		√
Baker (DB26)	Tundra	26-Apr-07	64.41800	96.40628	√	√	√	√	√	

### 3 Measurements

At the 45 sites marked in Figure 1, we measured snow depth, density, snow water equivalent (SWE), stratigraphy, and grain size. Our goal was to make measurements at paired sites, one on tundra (land) and one on ice (lake or river ice, depending on what was available: see the Description column in Table 1). It was not always possible to achieve this goal. At selected sites we collected snow samples for analysis of soot content, ionic loading, and mercury (Table 1). These chemical samples were collected on behalf of other research groups. The results will be analyzed and reported elsewhere, but the observed values, by site, appear in Appendices C, D, and E.

Standard methods were used to measure snow stratigraphy, density, and SWE (Colbeck et al. 1992). More extensive depth transects were measured than is customary by using a self-recording snow depth probe (U.S. Patent No. 5864059; *cf.* Sturm and Liston 2003) linked to a GPS. At most sites, 201 depth measurements were made at 0.5-m spacing over a 100-m line. These closely spaced measurements were followed by several hundred more measurements made at random spacings, their locations recorded by the GPS. Bulk SWE and density were determined from snow cores (measured in pairs) taken every 25 m along the sampling line. An ESC-30 snow corer (cross sectional area of 30 cm<sup>2</sup>) was used for these measurements. Grain size was measured using a stereo-microscope and comparator card. In addition, near-infrared (NIR) images of snowpit faces were made using a Sony DSC-P200 Cybershot 7.2-Mpixel digital camera equipped with an NIR filter (MaxMAX Xnite 850). These were processed in accordance with the methods of Matzl and Schneebeli (2007).

## 4 Results

### General Nature of the Snowpack

With the exception of a single site that was in the taiga forest, all of the snow examined during the traverse could be classified as tundra snow (Sturm et al. 1995). The tundra snow cover is a thin snowpack that consists mainly of wind slab and depth hoar (the latter usually making up layers at the bottom of the pack), with small but variable amounts of new and recent snow at the top of the pack. Features associated with wind deposition and erosion (dunes, sastrugi) are ubiquitous. As suggested in Figure 2, the mature tundra snowpack rarely has more than five to eight layers, a product of a limited number of winter precipitation events. Minus a thin veneer of new recent snow, the top layers are wind slabs due to the free play of the wind during the long winter, and the basal layers are depth hoar due to the strong gradients imposed by the frigid air temperatures. Wind slabs formed in early winter often completely metamorphose into depth hoar by the end of the season due to these gradients.

Tundra snow occurs throughout the tundra regions of the Arctic. Consequently, the snow cover observed on the traverse was similar to the snow cover of northern and western Alaska (Benson 1969, Benson and Sturm 1993, Sturm and Liston 2003), northern Manitoba (Derksen et al. 2003, 2005) and eastern Canada (Granberg 1978). One unintended but interesting result of the traverse is that the measurements confirm that this tundra snow can be found in a broad band stretching over 6000 km from Pt. Lay, Alaska, to Cape Dyer on Baffin Island. One feature of this type of snowpack that is not widely understood is that wind slab layers low in the pack (formed in early winter) completely metamorphose into depth hoar by the end of the winter. The grains in these layers are morphologically similar to regular depth hoar, but the layers are stronger and more cohesive than normal for depth hoar layers, a relict feature of the original wind slab. We call these layers “indurated.”

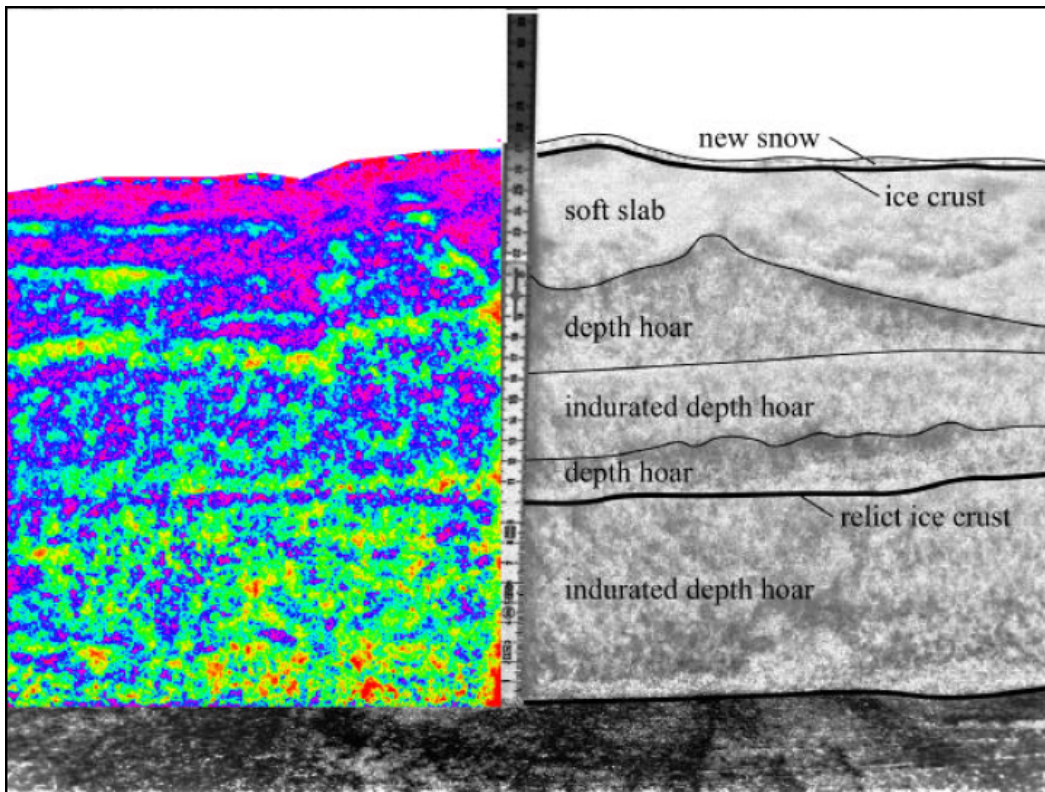
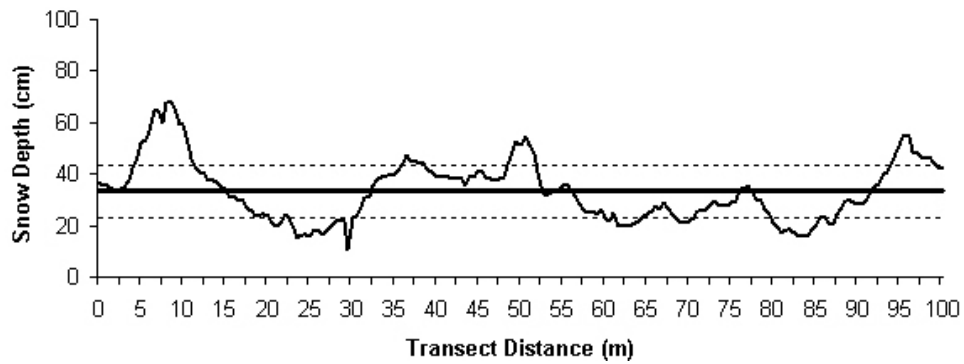


Figure 2. Snow stratigraphy (right) at site KD-7 (Yamba Lake). The color representation of the NIR image of the left side of the snowpit indicates the relative grain size (yellow and red = largest; purple and blue = smallest).

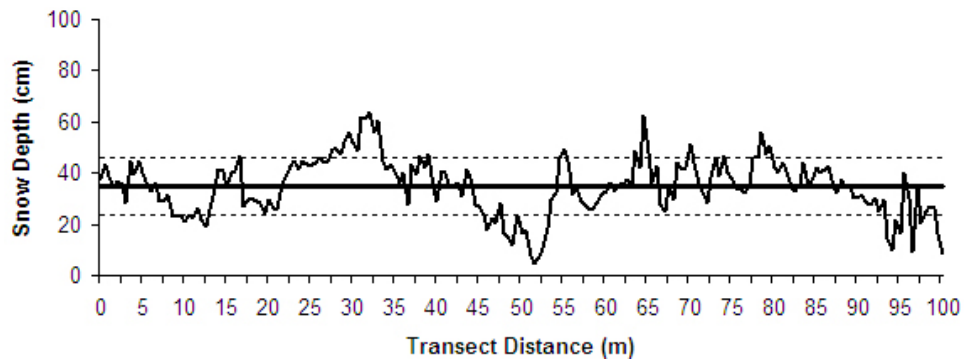
### Distributions of Depth, Density, and SWE

Typical snow depth transect profiles (100 m long) from the traverse are shown in Figures 3a and 3b for lake and tundra sites, respectively. The more spatially expansive roving snow depth measurements for the same sites are shown in Figures 3c and 3d. Similar profiles were obtained at all stations (Figure 1 and Table 1). Greater depth variability over land surfaces compared to lakes is evident in Figure 3, a finding that has been reported before (Sturm and Liston 2003, Derksen et al. 2005).

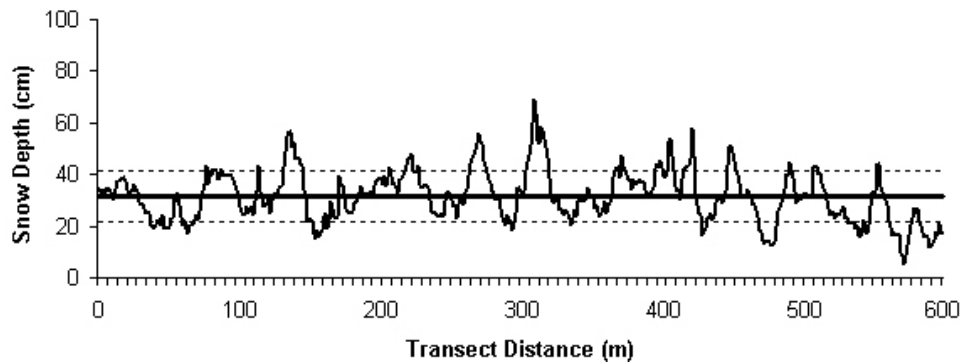
Probability distribution functions (PDFs) of snow depth, density, and SWE measurements based on all measured profiles are shown in Figures 4, 5, and 6, respectively. Statistics describing these PDFs are given in Table 2.



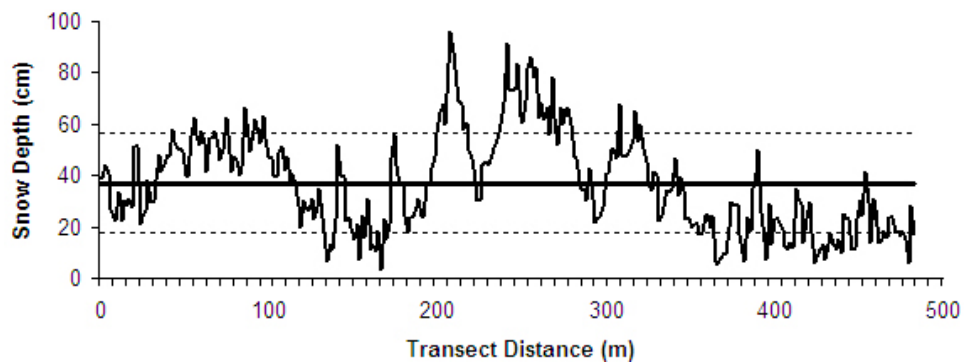
a. Typical 100-m snow depth profile for a lake site.



b. Typical 100-m snow depth profile for a tundra site.



c. Roving snow depth profile for a lake site.



d. Roving snow depth profile for a tundra site.

Figure 3. Typical snow depth profiles for lake and tundra sites. The mean value is shown by the heavy black line; dashed lines indicate  $\pm 1$  standard deviation.

Table 2. Summary of measured depth, density, and SWE probability distribution functions (see Figures 4–6). Automatic depth probes could only measure up to 122 cm deep, but not deeper, hence the uncertainty in max. and range values.

	Depth (cm)			Density (g/cm <sup>3</sup> )			SWE (mm)		
	All	Tundra	Lakes	All	Tundra	Lakes	All	Tundra	Lakes
Mean	33.1	38.9	29.2	0.356	0.347	0.379	108.7	119.9	100.7
St. Dev.	16.2	19.5	10.4	0.066	0.055	0.065	49.6	55.8	40.1
Min	0.2	0.2	0.4	0.207	0.207	0.227	12.0	18.8	12.0
Max	>122	>122	73.9	0.627	0.627	0.559	272.0	272.0	231.0
Range	>122	>122	73.5	0.420	0.420	0.332	260.1	253.2	219.0
CV	0.49	0.50	0.36	0.19	0.16	0.17	0.46	0.47	0.40
Skew	1.21	0.78	0.00	0.55	1.22	0.18	0.57	0.33	0.56
Kurtosis	2.99	1.31	-0.23	0.95	5.04	0.30	-0.04	-0.46	0.44

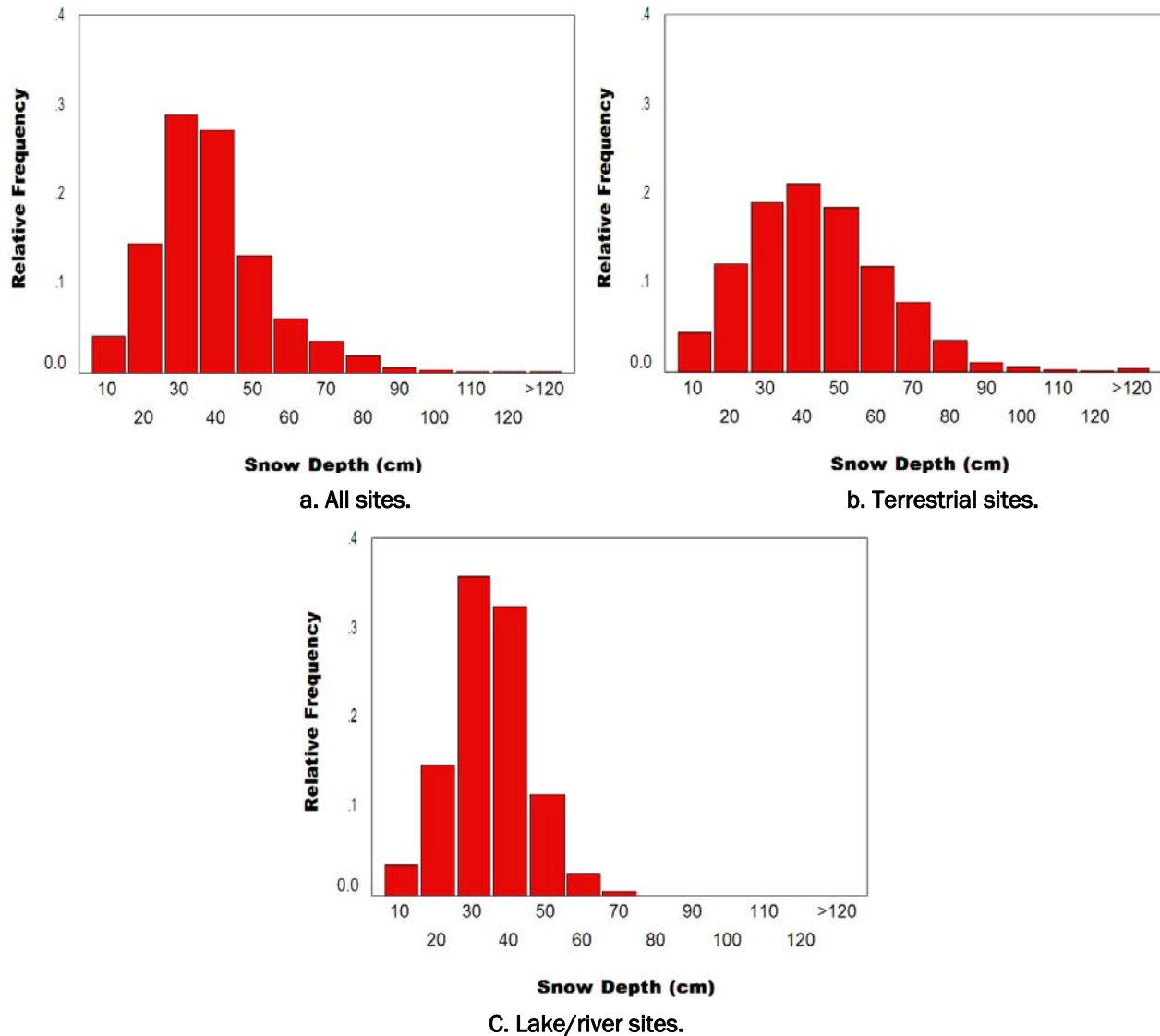


Figure 4. PDFs of measured snow depth.



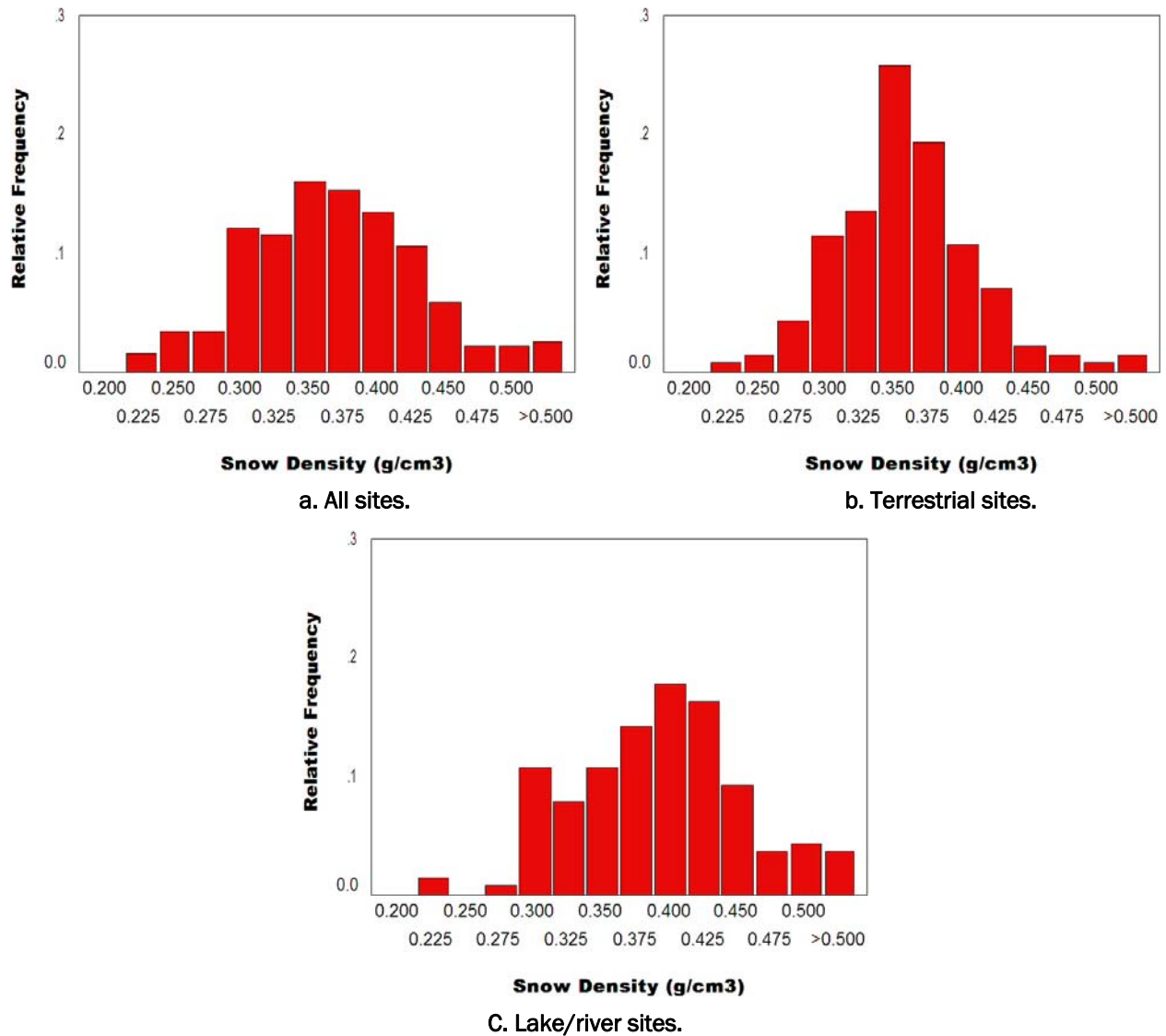


Figure 5. PDFs of measured bulk density.

Separate PDFs were plotted for all sites, terrestrial sites, and lake/river sites. For snow depth, all distributions have a peak at approximately 30–40 cm, but differences are clear between terrestrial sites (Fig. 4b) and lake sites (Fig. 4c). Snow depth range and variability were higher at terrestrial sites: the more extensive right skew was driven by variability in snow catchment and retention related to slope and vegetation. These two parameters are absent on lakes, where accumulation patterns are produced solely by wind drifting (Sturm and Liston 2003).

Unlike snow depth, the snow density measured on lakes (Fig. 5c) had a more uniform distribution (i.e., the probability of a bulk density of 0.3 was not significantly different than the probability of density of 0.4) compared

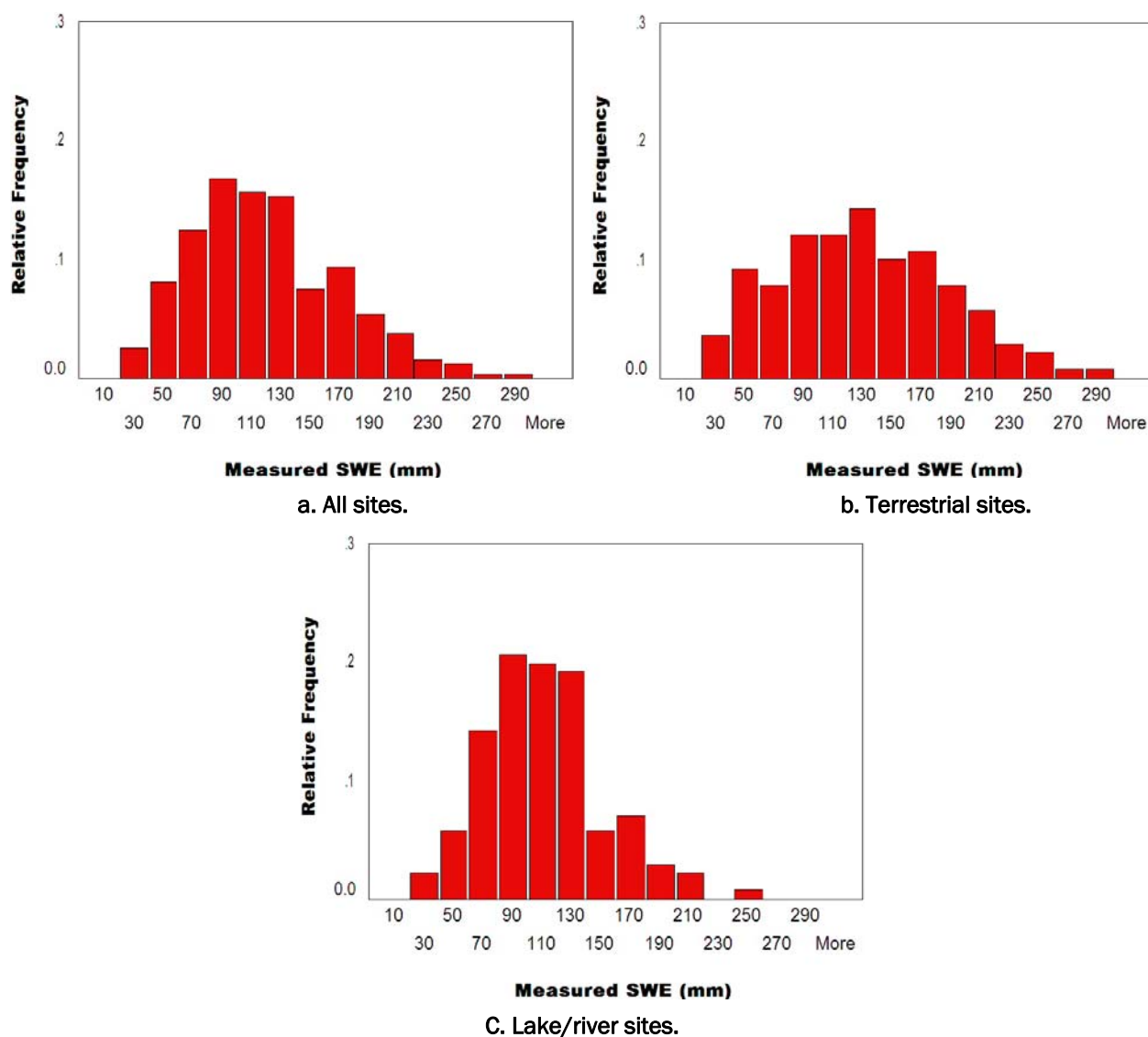


Figure 6. PDFs of measured SWE.

to terrestrial sites (Fig. 5b), which had a normal distribution centered on 0.35. The PDFs illustrate a clear lower threshold in snow density across the entire region of  $0.3 \text{ g/cm}^3$ . Measurements below this value were very rare (approximately 5% of all density measurements) regardless of land cover and substrate. Measured SWE values exhibited greater variability at terrestrial sites (Fig. 6b) versus lake sites (Fig. 6c). The trapping influence of vegetation creates the strong right skew in the terrestrial measurements, while a SWE storage capacity on lakes of approximately 130 mm was evident.

Because SWE is a product of depth and density, the underlying driver of SWE variability can be determined from the PDFs in Figures 4 and 5. On

land, a log-normal distribution for depth was coupled with a sharply peaked density PDF centered on about 0.35. Land snow depths varied with the distribution of tussocks, rocks, and shrubs, possibly even with the micro-topography, but the bulk density was consistent because wind action was the same across all of the vegetation and terrain types. This produced a broad, skewed SWE PDF (Fig. 6b). In contrast, without any shrubs or tussocks, the snow on the lakes and rivers tended to have a uniform depth due to much more consistent, uninterrupted wind action, but the same processes produced a wide range in density due to the successive pattern of hard-packed drifts interspersed with soft snow. For lakes, this density variation broadened the SWE distribution in comparison to the strongly peaked depth distribution. In short, tundra SWE is variable because tundra snow depth is variable (density is relatively constant), while lake/river SWE is variable because lake/river ice snow density is variable (though depth is relatively consistent).

We have compared the depth results shown here from Northwest Territories and Nunavut with results from previous traverses from northwest Alaska (Fig. 7 a, b, and c) (Sturm and Liston 2003) and northern Manitoba (also tundra snow: Fig. 7 d) (Derksen et al. 2005, updated with unpublished data). The results are qualitatively similar, particularly for terrestrial sites, though the Alaskan measurements show a larger modal range. It is possible that this larger modal range arises because the Alaskan data were taken on a south-to-north transect about 1000 km in length. Latitudinal gradients in precipitation and wind across this transect may be larger than those gradients found along the transect described here, which ran basically west to east.

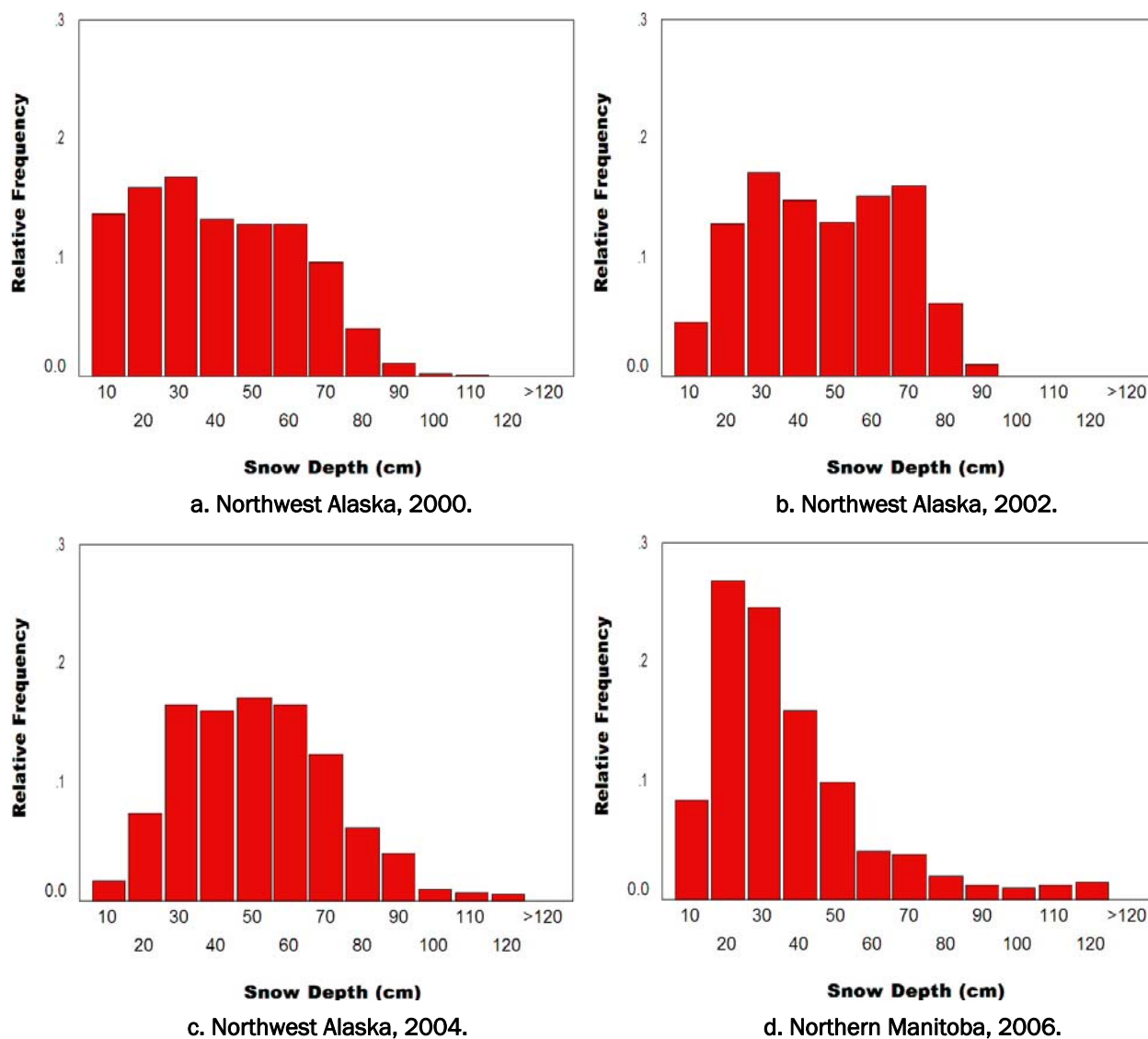


Figure 7. PDFs of measured snow depths from previous traverses.

## Stratigraphy

Snowpits were excavated to determine the snowpack stratigraphy at each site. Layer and grain types were noted following the classification of Colbeck et al. (1992) as outlined in Table 3. Because depth hoar and wind slab are ubiquitous in the tundra snow, the classification system was broadened for those types of snow to allow for a more nuanced approach. Specifically, in the field we recognized four types of slabs (soft, moderate, hard, and very hard) based on hardness, and we also noted depth hoar layers whose texture indicated they had origins as a wind slab. This type of layer is generally not seen outside of the Arctic. It arises in the Arctic because the temperature gradients are so strong (Sturm et. al. 1995) that

Table 3. Overview of snow grain classification used during the traverse.

Grain Type	Code	Grain Type	Code
New	1	Chains of hoar	11
Recent	2	Chains of hoar, indurated	12
Fine grains	3	Chains of hoar, voids	13
Medium grains	4	Icy hoar	14
Soft slab	5	Snow ice	15
Moderate slab	6	Ice layer	16
Hard slab	7	Melt grain clusters	17
Very hard slab	8	Melt grain clusters with percolation columns	18
Slab-to-hoar	9	Slab-to-hoar, slablike	19
Depth hoar	10	Solid hoar	20

even dense, fine-grained layers of wind slab eventually metamorphose into large, faceted, and striated depth hoar grains. A key characteristic of these slab-to-hoar layers is that they are tough, not fragile like most depth hoar. If comprised of mainly depth hoar crystals, yet still cohesive, we called the layers “indurated.” If a significant number of small wind grains remained, we called them “slablike.”

Of special stratigraphic note: at over 50% of the sites we visited there was a distinctive ice layer near the surface of the pack. On April 6 a rain-on-snow event was observed in the vicinity of Daring Lake, NWT. This event produced a surface ice crust or glaze that extended from Daring Lake east more than 100 km. Where exposed at the surface, this crust produced a shiny firnspiegel layer (Fig. 8) that at times was so slippery that it was treacherous to walk on. (This feature will be discussed in more detail later.)

As we have noted before for Alaskan tundra snow (Benson 1969, Benson and Sturm 1993), the snowpack of NWT and Nunavut was made up of a limited number of layers, almost always less than seven (Table 4). There were generally more layers on the tundra (terrestrial) than on ice (lake/river) substrates, probably because early season snowfalls fell into the water on lakes and rivers but were preserved on the tundra. In all locations, more than two thirds of the pack by thickness was depth hoar (including slab-to-hoar), while a surprisingly low percentage (11–14%) was wind slab. In northwest Alaska, more typically we have seen about twice this percentage of wind slab. We do not know whether 2007 was a low wind year in Nunavut and NWT, or whether depth hoar metamorphism driven by low temperatures converted more slabs into hoar, or some combination of both; however, as we discuss later, there is some reason to



Figure 8. Firnspiegel (icy, shiny snow) produced by the April 6<sup>th</sup> rain-on-snow event.

think that metamorphism was more extreme over the traverse route than in northwest Alaska. The contrast in bulk density between tundra and lake sites was expected (windier lakes equal more dense snow layers, hence overall a denser snowpack), but the low density for river sites is more difficult to explain. Despite these minor differences, overall, we suggest that the snow across all terrain units sampled during the traverse tended to be similar. All of it was thin, with relatively few layers, and almost all of it was fully converted into coarse-grained depth hoar by the end of the winter. Table 5 provides the full data that are summarized in Table 4.

Table 4. Stratigraphy statistics.

	All Sites	Tundra Sites	Lake Sites	River Sites
Number of Layers	5.8	6.6	4.9	5.5
Ave. Layer Thickness (cm)	6.6	6.7	6.4	6.3
Total Thickness (cm)	37.1	43.4	30.1	33.6
SWE (cm)	11.4	14.0	10.1	8.1
Bulk density (g/cm <sup>3</sup> )	0.311	0.319	0.340	0.236
Hoar Fraction	0.71	0.65	0.76	0.71
Slab Fraction	0.12	0.14	0.11	0.12
Icy Fraction	0.03	0.02	0.04	0.02
New/Recent Fraction	0.11	0.14	0.07	0.12
Other Fraction	0.03	0.03	0.02	0.03

Table 5. Summary of snowpack stratigraphic composition by site.

Site	Description	Number of Layers	Ave. Layer Thickness (cm)	Total Thickness (cm)	SWE (cm)	Bulk Density (g/cm <sup>3</sup> )
Yukon	River	4	8.3	33	6.0	0.183
Porcupine	River	6	5.3	32	5.9	0.185
Mackenzie	River	6	6.8	41	7.6	0.187
Deline	Lake	6	8.0	48	9.0	0.188
Great Bear 1	Lake	4	5.5	22	5.6	0.254
Great Bear 2	Lake	7	5.1	36	9.7	0.270
Great Bear 3	Lake	6	3.8	23	7.3	0.316
Great Bear 4	Lake	4	7.0	28	11.8	0.422
Great Bear 5	Lake	2	11.5	23	10.7	0.465
Dease	River	6	5.7	34	8.3	0.244
Bloody Falls	Tundra	6	7.0	42	11.5	0.274
KD1	Tundra	7	5.0	35	11.3	0.323
KD2	Lake	4	4.5	18	5.6	0.309
KD3	Lake	5	4.1	21	7.8	0.382
KD4	Lake	6	5.0	30	10.7	0.358
Rockinghorse	Lake	5	6.4	32	10.2	0.320
KD6	Tundra	6	8.7	52	18.8	0.361
Yamba	Lake	7	4.0	28	8.0	0.287
Lake Providence	Tundra	8	4.0	32	8.4	0.261
Diavik	Tundra	5	6.0	30	10.4	0.346
Lac de Gras	Lake	7	5.1	36	13.4	0.372
Thonokied Lake	Lake	5	6.6	33	11.2	0.340
Thonokied	Tundra	5	11.0	55	17.2	0.313
Aylmer Lake	Lake	5	6.4	32	10.5	0.327
Aylmer/Clinton-Colden	Tundra	8	5.5	44	15.8	0.359
Clinton-Colden Lake	Lake	4	12.5	50	20.0	0.400
Clinton-Colden	Tundra	5	4.6	23	8.0	0.349
Sifton Lake	Lake	5	6.2	31	11.3	0.363
North Hanbury	Tundra	7	4.4	31	9.0	0.289
West Hoare	Tundra	7	9.0	63	22.8	0.362
Hoare Cabin	Tundra	6	6.0	35	9.7	0.276
Hoare Lake	Lake	5	6.2	31	10.0	0.324
Hanbury/Thelon	Tundra	7	6.4	45	13.7	0.305
Hornby Point	Forest	9	9.9	89	19.6	0.220
Hornby Thelon River	River	4	5.8	23	4.9	0.212
Thelon Nunavut	River	6	6.8	41	12.5	0.304
Thelon Lookout Point	River	7	3.1	22	5.3	0.239
Lookout Point	Tundra	5	10.2	51	18.2	0.356
Thelon Cabin	Tundra	8	5.1	41	11.7	0.285
Beverly Lake	Lake	4	8.0	32	11.6	0.364
Aberdeen	Tundra	8	5.9	47	13.5	0.286
Aberdeen Lake	Lake	3	6.3	19	7.7	0.406
South Schultz	Tundra	9	8.8	79	27.1	0.344
North Baker	Tundra	5	6.4	32	10.9	0.340
Baker	River	5	8.6	43	14.5	0.336
<b>Average</b>	<b>All</b>	<b>5.8</b>	<b>6.6</b>	<b>37.1</b>	<b>11.4</b>	<b>0.311</b>
<b>Average</b>	<b>Tundra</b>	<b>6.6</b>	<b>6.7</b>	<b>43.4</b>	<b>14.0</b>	<b>0.319</b>
<b>Average</b>	<b>Lake</b>	<b>4.9</b>	<b>6.4</b>	<b>30.1</b>	<b>10.1</b>	<b>0.340</b>
<b>Average</b>	<b>River</b>	<b>5.5</b>	<b>6.3</b>	<b>33.6</b>	<b>8.1</b>	<b>0.236</b>

Table 5 (cont). Summary of snowpack stratigraphic composition by site.

Site	Description	Fraction (%)					Grain Long	Grain Short
		Hoar	Slab	Wet/Icy	New/Recent	Other		
Yukon	River	97.0	0.0	0.0	3.0	0.0	4.3	2.2
Porcupine	River	46.9	12.5	0.0	21.9	18.8	4.6	1.7
Mackenzie	River	46.3	26.8	2.4	24.4	0.0	4.9	1.6
Deline	Lake	83.3	0.0	2.1	14.6	0.0	9.1	3.6
Great Bear 1	Lake	81.8	0.0	0.0	18.2	0.0	3.8	0.5
Great Bear 2	Lake	91.7	0.0	8.3	0.0	0.0	5.5	1.4
Great Bear 3	Lake	90.9	0.0	9.1	0.0	0.0	3.0	1.0
Great Bear 4	Lake	96.4	0.0	3.6	0.0	0.0	2.8	1.0
Great Bear 5	Lake	97.8	0.0	0.0	2.2	0.0	2.0	1.0
Dease	River	79.4	0.0	8.8	11.8	0.0	5.3	0.9
Bloody Falls	Tundra	66.7	0.0	16.7	0.0	16.7	3.9	0.7
KD1	Tundra	60.0	32.3	2.0	5.7	0.0	5.5	1.6
KD2	Lake	94.4	0.0	0.0	5.6	0.0	3.4	1.8
KD3	Lake	57.6	39.0	3.4	0.0	0.0	2.7	0.7
KD4	Lake	66.7	0.0	0.0	3.3	30.0	2.9	1.2
Rockinghorse	Lake	62.5	29.7	1.6	6.3	0.0	0.9	0.3
KD6	Tundra	76.9	17.1	0.2	5.8	0.0	2.3	0.6
Yamba	Lake	75.0	20.7	0.7	3.6	0.0	2.8	0.5
Lake Providence	Tundra	84.4	0.0	0.6	6.3	8.8	1.8	0.5
Diavik	Tundra	83.3	12.7	0.7	3.3	0.0	3.8	0.6
Lac de Gras	Lake	58.3	41.7	0.0	0.0	0.0	2.4	0.5
Thonokied Lake	Lake	99.1	0.0	0.9	0.0	0.0	3.5	0.9
Thonokied	Tundra	45.5	41.8	0.0	0.0	12.7	3.6	0.7
Aylmer Lake	Lake	75.0	15.6	0.0	0.0	9.4	3.5	0.4
Aylmer/Clinton-Colden	Tundra	40.9	45.0	0.5	6.8	6.8	2.7	0.8
Clinton-Colden Lake	Lake	91.6	0.0	0.4	8.0	0.0	2.2	0.1
Clinton-Colden	Tundra	65.2	0.0	13.0	21.7	0.0	2.5	0.4
Sifton Lake	Lake	50.0	0.0	43.5	6.5	0.0	4.2	0.3
North Hanbury	Tundra	63.9	33.9	0.6	1.6	0.0	2.2	0.8
West Hoare	Tundra	93.7	0.0	3.2	3.2	0.0	4.1	0.6
Hoare Cabin	Tundra	48.0	0.0	0.6	37.1	0.0	1.3	0.5
Hoare Lake	Lake	73.5	19.4	0.6	6.5	0.0	1.8	3.7
Hanbury/Thelon	Tundra	48.9	20.0	0.0	26.7	4.4	2.2	1.4
Hornby Point	Forest	71.9	15.7	1.1	11.2	0.0	3.0	1.1
Hornby Thelon River	River	89.1	8.7	2.2	0.0	0.0	5.4	1.1
Thelon Nunavut	River	68.3	29.3	2.4	0.0	0.0	9.0	1.1
Thelon Lookout Point	River	85.5	9.1	0.9	0.0	4.5	6.2	0.4
Lookout Point	Tundra	62.7	11.8	0.0	25.5	0.0	2.1	0.6
Thelon Cabin	Tundra	80.5	9.8	0.0	1.2	8.5	3.6	0.6
Beverly Lake	Lake	15.6	50.0	0.0	34.4	0.0	1.8	0.3
Aberdeen	Tundra	68.1	0.0	0.0	31.9	0.0	3.8	0.6
Aberdeen Lake	Lake	78.9	0.0	0.0	21.1	0.0	1.6	0.4
South Schultz	Tundra	61.8	6.3	0.3	31.6	0.0	2.2	0.5
North Baker	Tundra	60.3	0.0	2.2	37.5	0.0	2.1	0.2
Baker	River	55.8	6.5	0.5	37.2	0.0	2.5	0.6
<b>Average</b>	<b>All</b>	<b>70.9</b>	<b>12.3</b>	<b>3.0</b>	<b>10.8</b>	<b>2.7</b>	<b>3.4</b>	<b>0.9</b>
<b>Average</b>	<b>Tundra</b>	<b>65.3</b>	<b>13.6</b>	<b>2.4</b>	<b>14.5</b>	<b>3.4</b>	<b>2.9</b>	<b>0.7</b>
<b>Average</b>	<b>Lake</b>	<b>75.8</b>	<b>11.4</b>	<b>3.9</b>	<b>6.8</b>	<b>2.1</b>	<b>3.1</b>	<b>1.0</b>
<b>Average</b>	<b>River</b>	<b>71.0</b>	<b>11.6</b>	<b>2.2</b>	<b>12.3</b>	<b>2.9</b>	<b>5.3</b>	<b>1.2</b>



To look at the stratigraphy in more detail, we have separated the data into two categories: snowpits measured on tundra (terrestrial), and snowpits measured on lake and river ice.

In both cases, the components of the pack were depth hoar (more or less indurated, depending on origin), wind slabs (harder or softer, depending on deposition conditions), new/recent snow (highly dependent on recent wind events), and icy snow. Other than the differences in thickness and density noted in Table 4, there were virtually no statistical differences in the stratigraphy based on the substrate. Allowing for differences in the total number of tundra versus ice snowpits, wind slabs, depth hoar, indurated depth hoar, and slab-to-hoar textures were observed as frequently on the tundra as on lakes and rivers. As we show below, grain sizes and layer hardnesses were also the same over ice as over tundra. Nevertheless, perusal of the NIR photos suggest that the transformation of slabs into depth hoar was in general more complete over an ice substrate. This is illustrated in Figure 9, where side-by-side NIR images from a tundra and lake pair of snowpits shows more distinct (less metamorphosed) layers on the tundra than on the ice. These textural differences were subtle and not captured in the layer classifications done in the field, but they may be real.

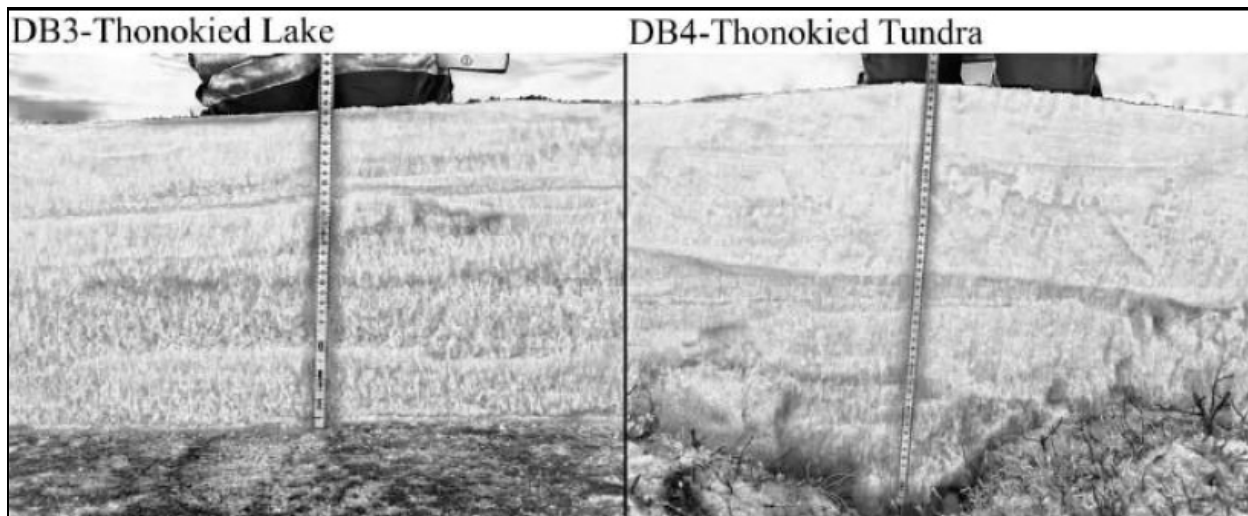


Figure 9. NIR snow stratigraphy photographs for a pair of adjacent lake and tundra sites, showing coarser grains (more depth hoar metamorphism) and less distinct layers on the lake than on the tundra.

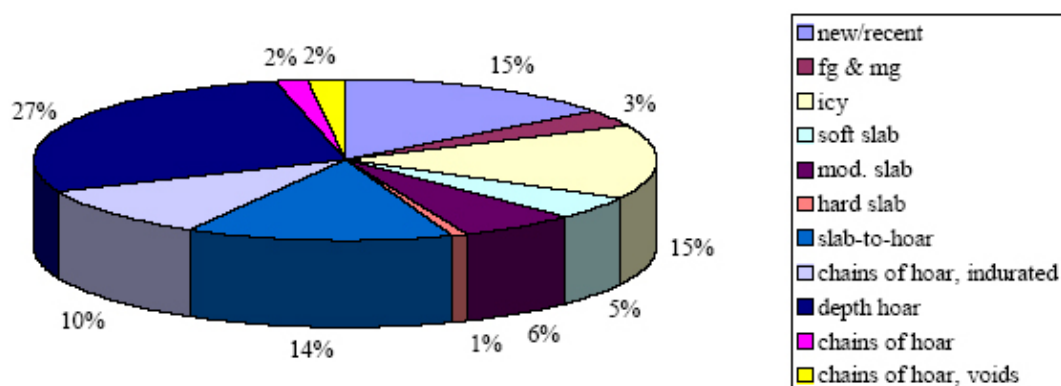
Two of the snow textures (new/recent and icy) tend to change rapidly in response to weather events and by thickness were not major components of the snowpack. What little new/recent snow was present (Table 4: ave.

11% of total pack by thickness) most often was observed to be an ephemeral layer at the top. As soon as the wind started to blow, the thickness of this layer could double, or it could go to zero, a process we watched in action many times. If the last six sites of the traverse (Table 5) are excluded (each of which was about 30% new/recent snow because of a snowstorm), the average percentage of new/recent across the traverse falls to 7.5% of total. While new snow is important in many ways, it is a transient feature of the snowpack and therefore hard to predict in time and space. Icy snow was even a smaller percentage of the pack by thickness, on average 3%. The only exception was on Sifton Lake, where overflow had formed a substantial layer of snow ice at the base of the pack. In general, we found overflow and snow ice to be rare. Most of the other icy layers in the snowpack were the product of a single warm period with rain on snow. These layers were never more than 5 mm thick, though as we discuss later, they may have radiometric importance.

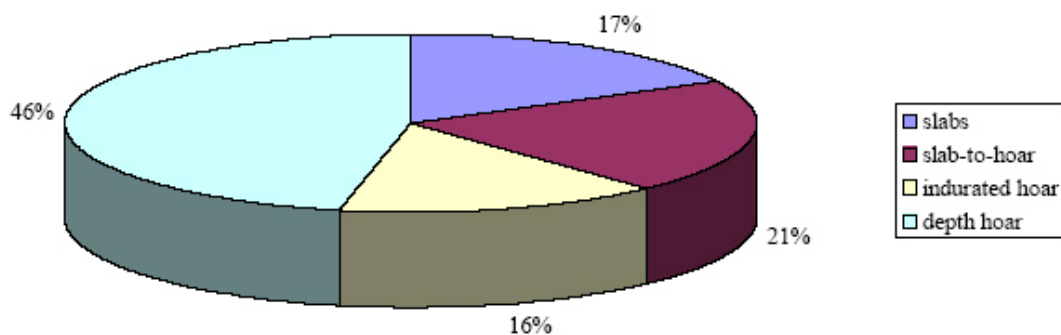
Excluding new/recent and icy snow, we now examine the relative distribution of depth hoar layers and wind slabs. These account for almost 80% by thickness of the pack. The key to understanding the stratigraphy observed on the traverse, and elsewhere in the Arctic on other traverses, is how these two basic types of snow textures play out. They are linked. As noted before, wind slabs can be converted into depth hoar, while depth hoar can be eroded and reconstituted as a wind slab. Strong winds and vigorous wind transport tend to form dense, tough slabs that resist depth conversion. Less strong winds form slabs that are less cohesive and fine-grained and that tend to metamorphose more easily. Early snow and low winter temperatures produce strong temperature gradients across the snowpack that can accelerate slab-to-hoar conversion; late snow and mild temperatures tend to preserve wind slabs.

Figure 10a shows the relative abundance (by count rather than thickness or SWE) of 11 types of snow seen in the 259 layers that were identified in the field. Thirty-three percent of all layers were neither depth hoar nor wind slab. If we remove these layers from the count [remove new, recent, medium and fine-grained (mg/fg) snow, melt clusters, and icy snow] and look at the remaining layers (Fig. 10b), a more interesting story appears. Forty-six percent of this remaining subset is classified as pure depth hoar. These are layers that probably did not start out as wind slabs. They were initially new, recent, or fine-grained snow layers. Seventeen percent was still wind slab at the time of the traverse. The remaining 37% was depth

hoar, with textural indicators suggesting that it had been transformed into depth hoar from wind slab. Adding this 37% to the 18% wind slab that remained suggests that 55% of the snowpack was initially wind slab. In essence, about half the snow started as non-wind-slab snow and became depth hoar, while the other half started as wind slab, but most of it metamorphosed into depth hoar. This initial distribution is consistent with tundra snow results from northwest Alaska (Sturm and Liston 2003; Fig. 2), where about half of the snow was wind slab, half depth hoar. The implication of this finding is that initial slab abundances across the traverse region were more typical of those found elsewhere in the Arctic, but that post-deposition metamorphism resulted in an unusually low percentage of slabs surviving until spring. While it is only speculation, this suggests that in the traverse region, conditions may favor even more extreme metamorphism than is typically found in arctic tundra snow.



a. Percentage of layers (by number of layers) for all layers (259).



b. Percentage of depth hoar and wind slab layers only.

Figure 10. Relative abundance of snow types by layer. Slab-to-hoar and indurated textures are derived from wind slabs.

We have tabulated grain size by snow layer type in Table 6. The values in the table are averages computed for all layers identified as that type of snow. There were 259 layers on which grain size was measured. The

percentages listed in Figure 10a, multiplied times 259, give the approximate  $n$ -value for each grain size average. Ice layers do not have distinct grains, so they have been excluded from the table. The results show that the largest grains were found in indurated depth hoar layers, as well as depth hoar chain assemblages, and that a) these grains were five times larger than the grains in wind slabs, and b) the hoar grains tended to be plate-like with short to long axial ratios near 1:4.

Table 6. Grain sizes (microscope and comparator card) by snow texture type. The hardness code is a relative measure of layer hardness: the higher the number, the harder the snow.

	Hardness Code	Grain Size Long Axis (mm)	Grain Size Short Axis (mm)
New/Recent	2.5	0.9	0.4
Fine & Medium Grained	4.6	0.9	0.4
Soft Slab	3.2	0.8	0.3
Mod. Slab	4.1	0.8	0.6
Hard Slab	5.0	2.0	0.3
All Slabs	3.8	0.9	0.5
Slab-to-Hoar	3.8	2.3	0.8
Indurated Hoar	3.5	5.7	1.1
Slab-to-Hoar & Indurated	3.7	3.8	0.9
Depth Hoar	2.5	4.0	1.1
Hoar Chains	2.3	6.4	1.6
Melt Clusters	3.6	1.3	0.5

We tested whether for any type of snow layer, the grain sizes differed if the snow was on tundra versus ice substrate but found no significant differences (Table 7).

Table 7. Grain size by snowpit substrate.

		Grain Size Long Axis (mm)	Grain Size Short Axis (mm)	Average Density
Slabs	Ice	1.2	0.6	0.4
	Tundra	0.7	0.4	0.4
Slab-to-Hoar	Ice	2.5	0.9	0.3
	Tundra	2.1	0.5	0.4
Depth Hoar	Ice	3.7	1.0	0.3
	Tundra	4.4	1.2	0.3
Indurated Hoar	Ice	5.6	1.2	0.3
	Tundra	6.2	0.8	0.3

## Density and SWE

From the single snowpit excavated at each site, mean snowpack density was determined by proportionally weighting the individual layer density measurements. These were compared to the average value determined from 12 direct measurements of bulk density made using the ESC-30 corer along the 100-m sampling line (Fig. 11). There was a tendency for the pit measurements to underestimate density relative to the full 100-m transect mean as measured with a corer. Major outliers at some lake and river sites strongly influenced the relationship, consistent with the finding in Figure 5 that lake density was more locally variable than tundra snow density. Strangely, normally, we have found that the core densities are lower than the ones determined from layer measurements (Sturm et al., in prep.).

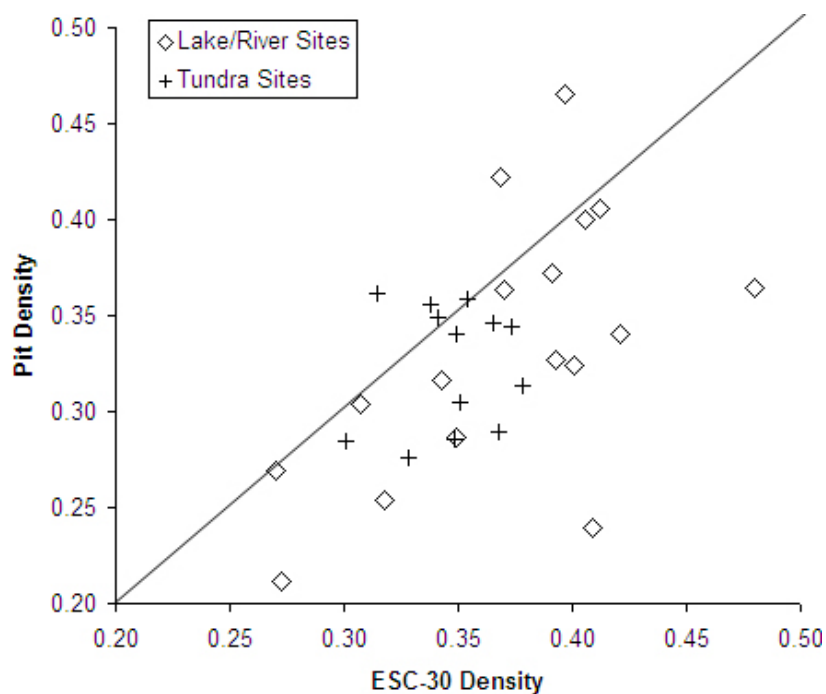
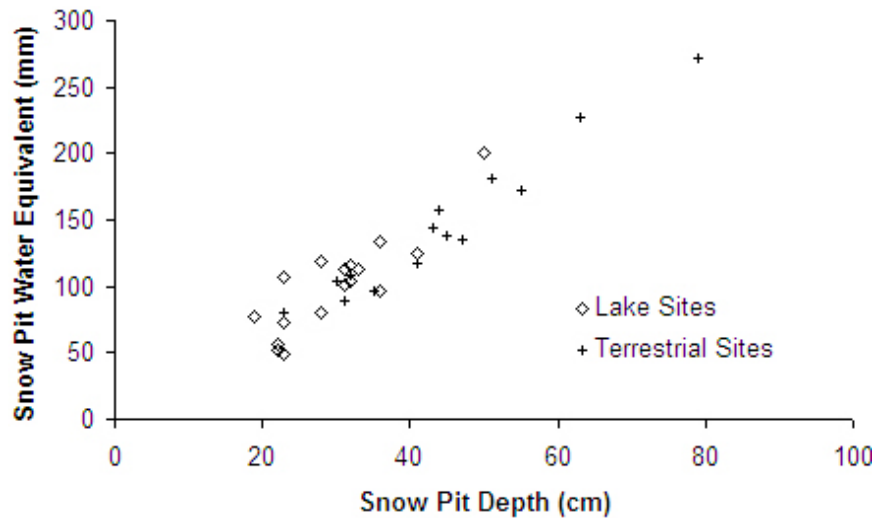


Figure 11. Comparison of mean pit density ( $n = 1$  at each site) with snow core density ( $n = 12$  at each site).  $r^2 = 0.27$ .

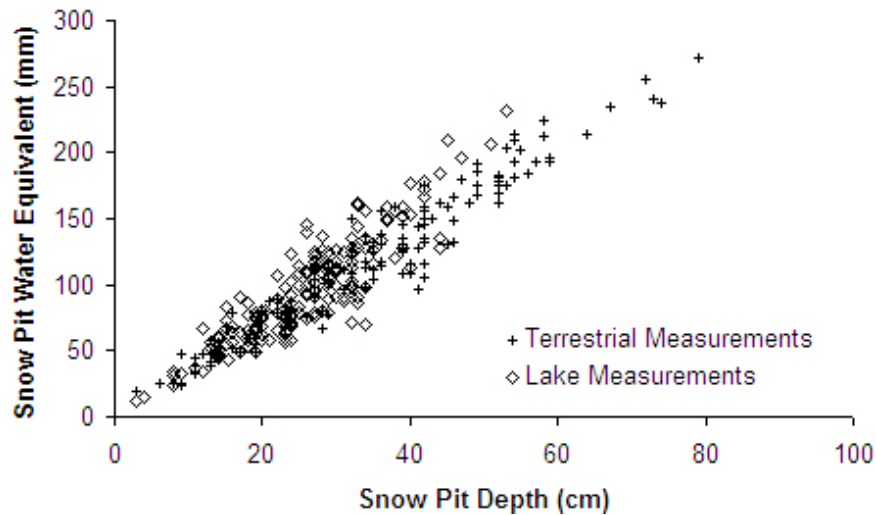
## SWE to Depth Relationship

SWE is the product of depth and density. Being able to infer SWE from a depth measurement is desirable, given the greater ease of acquiring depth versus snow core measurements. Sturm et al. (in review) examined a large dataset of historical measurement triplets (depth, density, SWE) from North America and Europe. From this 25,757-point dataset, it is clear that measurements of snow depth, coupled with contextual spatial and

temporal information (where and when were the measurements made), can produce reliable estimates of SWE based on linear depth versus SWE relationships. Depth and SWE measurements from snowpits (Fig. 12a) and ESC-30 measurements (Fig. 12b) from the traverse were plotted to examine how well these SWE-depth relationships were represented in this new dataset. As with the larger data set, there was a strong correlation between depth and SWE.



a. Snowpit measurements (overall  $r^2 = 0.90$ ).



b. ESC-30 measurements (terrestrial  $r^2 = 0.94$ ; lake  $r^2 = 0.78$ ).

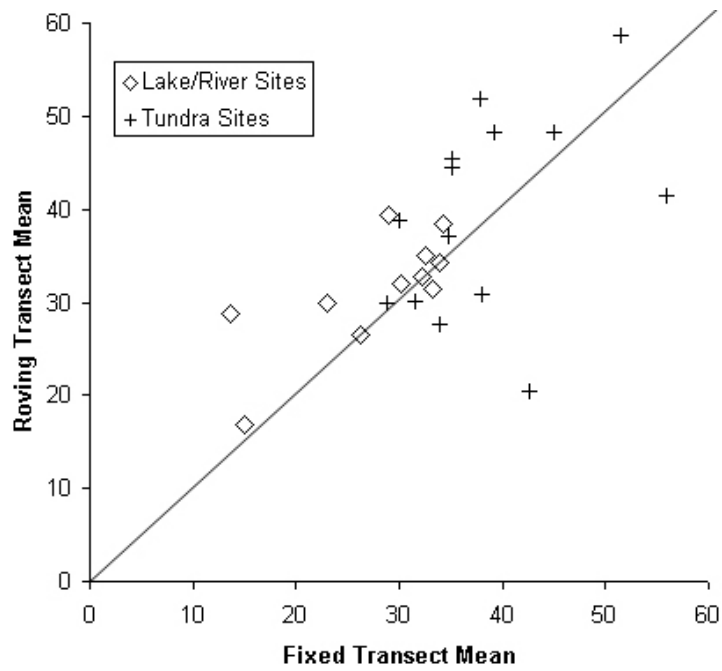
Figure 12. SWE versus depth.

## Fixed Transect vs. Roving Transects

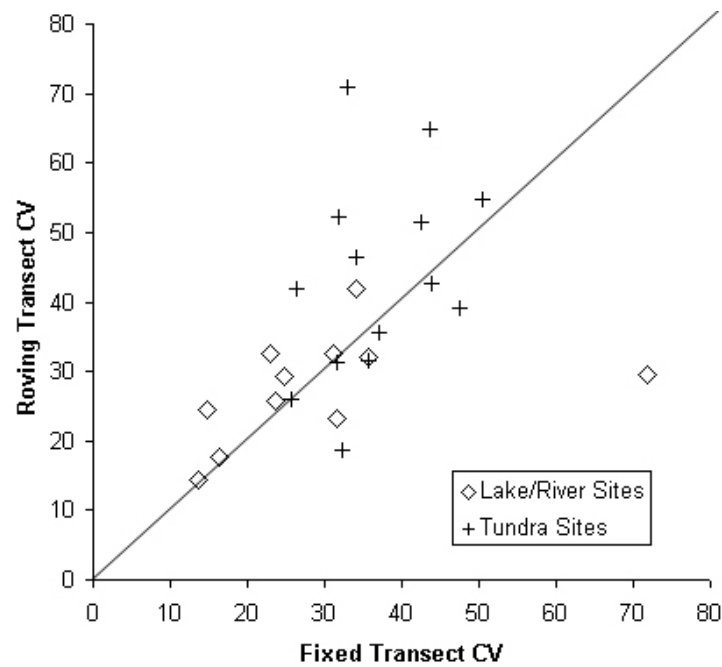
At each site, depth probe and ESC-30 SWE/bulk density measurements were made at fixed intervals (every 50 cm for depth; 25 m for SWE) along a 100-m marked transect (called here the *fixed* transect). Depth measurements were also acquired at irregular intervals (typically every two to three paces) along additional transects that extended away from the 100-m sampling line in order to capture the depth variability over a larger area (called here the *roving* transect). These two datasets allowed a number of sampling-related questions to be addressed:

- How well did the data from the fixed transects match the data from the roving transects?
- How similar were direct measurements of SWE (made using the ESC-30 along the fixed transect) with SWE estimates based on the roving depths and a fixed bulk density value?

Figures 13 and 14 show that the 100-m fixed transects tended to underestimate the mean depth (Fig. 13a) and SWE (Fig. 14a) relative to the roving transects, particularly for the lake and river sites. Essentially, there was a tendency for there to be more snow away from the 100-m transect, suggesting that our site selection choices (motivated by a desire to find consistent, “neutral,” flat tundra sites) were not truly random. Greater variability (reflected by higher CV values) was captured by the roving transect measurements of snow depth (Fig. 13b), but this systematic bias was not evident with SWE (Fig. 14b).



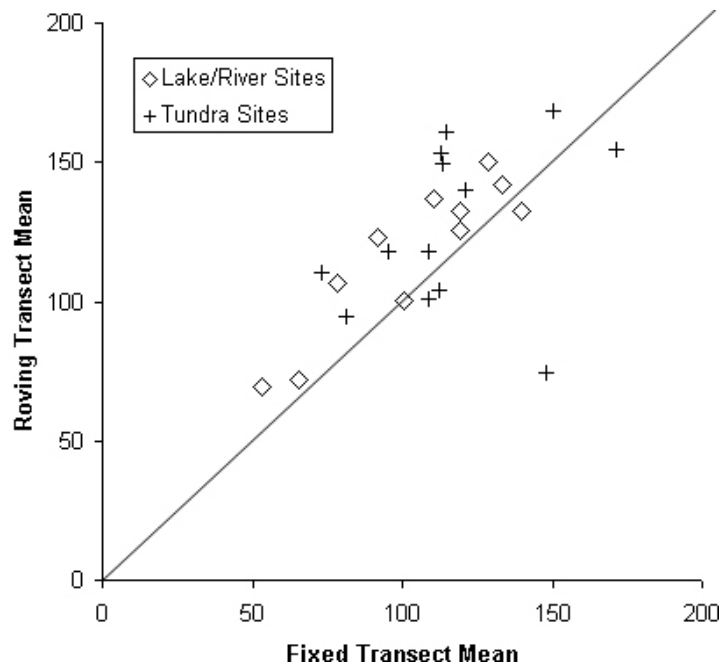
a. Mean fixed transect snow depths (cm) versus roving snow depth transects (also cm).



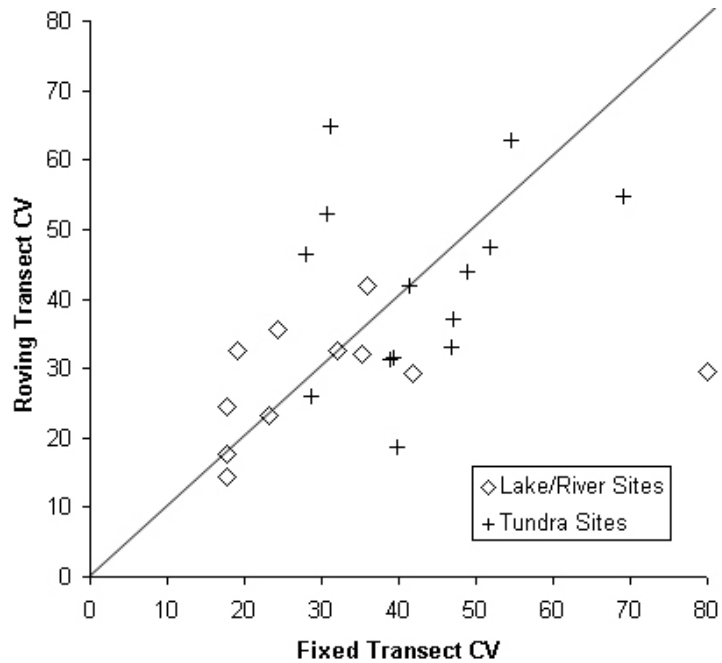
b. CV fixed transect snow depths (cm) versus roving snow depth transects (also cm).

Figure 13. Relationships between fixed and roving transect snow depths (mean and CV).





a. Mean fixed transect SWE measurements versus roving transect estimates of SWE (depth  $\times$  mean site density).



b. CV fixed transect SWE measurements versus roving transect estimates of SWE (depth  $\times$  mean site density).

Figure 14. Relationships between fixed and roving transect SWE (mean and CV).

## Longitudinal Gradients

The conventional wisdom is that snow varies along altitudinal and latitudinal gradients, but not necessarily along longitudinal gradients. Since the traverse was basically west to east, here we examine if there were any longitudinal gradients in the snow properties. Storm tracks and synoptic patterns for Northwest Territories and Nunavut are complex, so both latitudinal and east-west snow gradients across NWT and Nunavut are possible.

The most consistent period of sampling occurred during the Daring Lake to Baker Lake portion of the traverse (April 16 to 26). Sample sites were located at least every 1 degree of longitude (Fig. 15). We have used a correlation analysis of mean site values versus longitude to see if there are gradients reflected in the data. Two sites along the Thelon River were omitted from this analysis because the Thelon “Oasis” is known to be an anomalous area, a large outlier of taiga forest hundreds of kilometers north of the normal treeline.

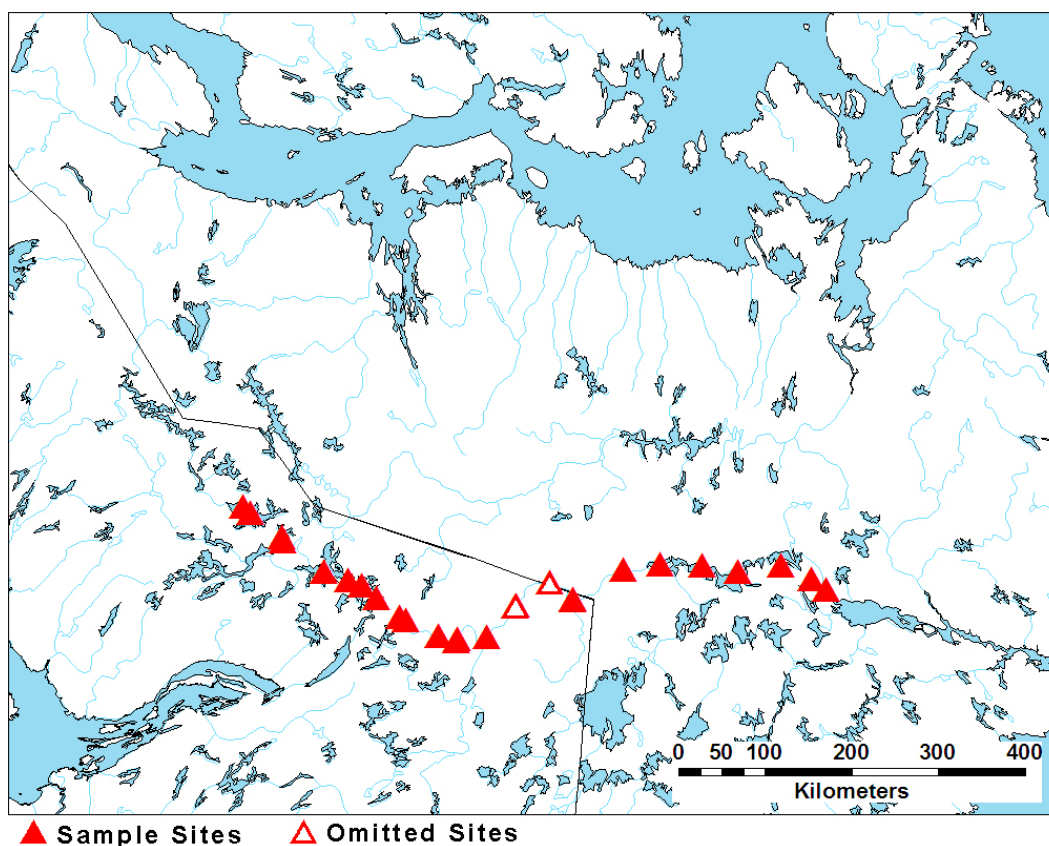


Figure 15. Sites used for analysis of longitudinal gradients.

The results show only weak relationships with longitude for the tundra sites (Table 8), though stronger relationships were evident for the lake sites. The snow cover on the lakes became shallower and more dense and was composed of fewer layers with smaller grains as we moved eastward.

**Table 8. Correlation results for snow parameters versus longitude.**

	Tundra	Lakes
Depth	-0.20	0.73
Density	0.18	-0.52
SWE	-0.10	0.52
Layers	-0.39	0.79
Grain Long	0.25	0.61

All measurements were also segmented into 1 degree longitudinal bins. Box plots of depth, density, and water equivalent are shown in Figure 16. No longitudinal trends in the variability of snow properties are evident for tundra and lake sites. The speculative depth, density, and SWE gradients for snow on lakes suggested by the correlation analysis are evident in the box plots, but these gradients are very subtle.

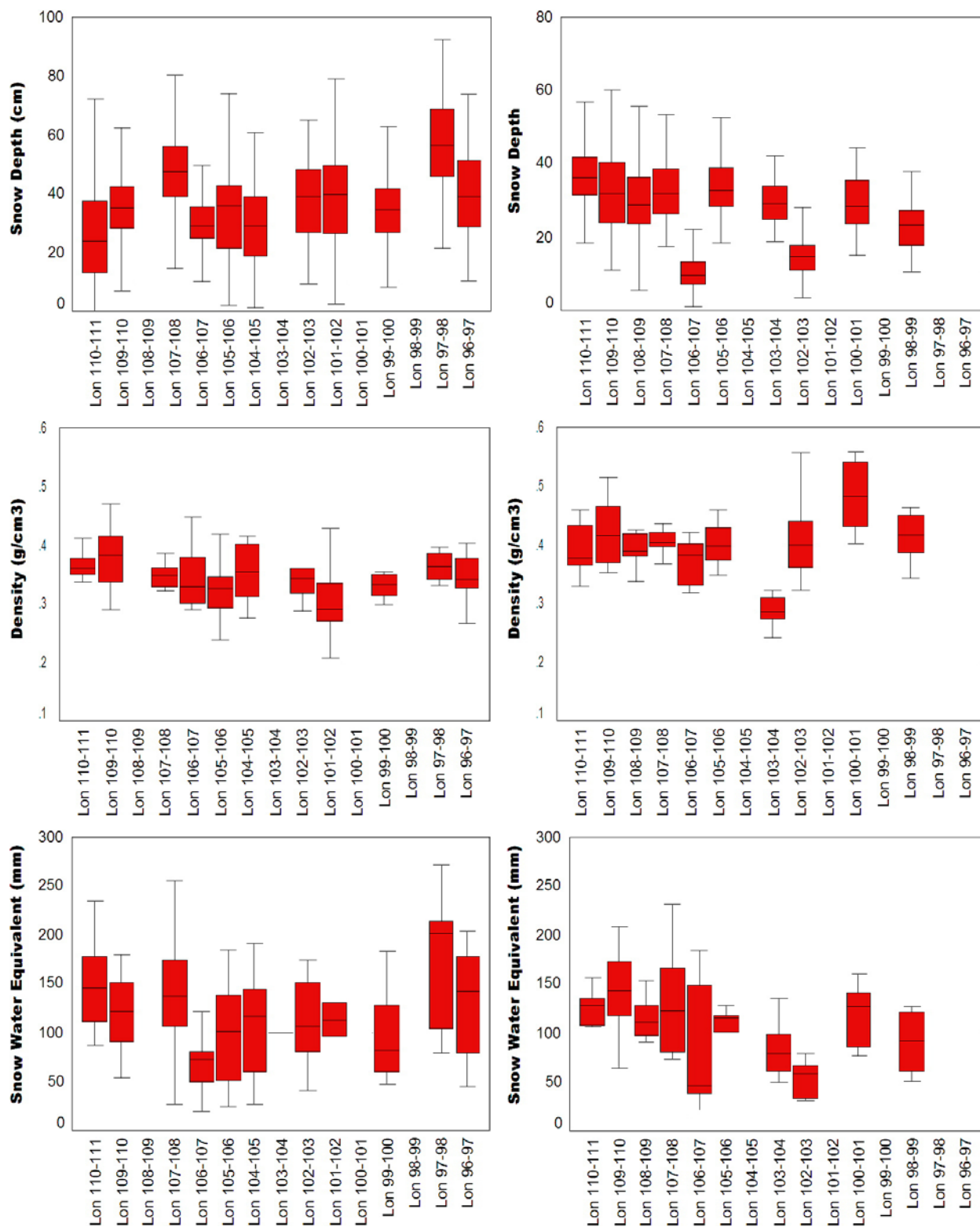


Figure 16. Longitudinal gradients in depth (top), density (middle), and SWE (bottom) for terrestrial (left) and lake (right) measurements.

## The Nature of the North American Tundra Snow Cover

The snow traverse described here caps more than a decade of intense measurements of the snow cover in arctic North America, though mostly in smaller, local areas. In Alaska, a series of over-snow traverses were begun in 1994 in the Kuparuk Basin. These were about 200 km in length. They were then extended to northwest Alaska in 2000, where snow along a 1000-km route between Nome and Barrow was measured. (Olsson et al. 2002, Liston and Sturm 2002, Sturm and Benson 2004, Douglas and Sturm 2004) In Canada, four years of intensive snow sampling to determine landscape controls on snow (re)distribution and provide ground measurements for comparison with satellite and airborne remote sensing data started at Daring Lake in 2003 (Rees et al. 2006). Other campaigns were conducted near Churchill, Manitoba.

Our most significant finding is that the snow cover across this 6000-km-wide region is quite similar from place to place. The depth distribution, the density, the stratigraphy, and the texture show more similarities than differences despite obvious spatial variability and landscape controls. The tundra snow cover (taiga snow is also common in the region but was not heavily sampled during the traverse), as we have shown here (and described elsewhere, Benson and Sturm 1993), is composed of two end-member types of snow: depth hoar and wind slab. The former is coarse grained, the latter fine grained. Due to wind action, the depth and thickness of individual layers vary markedly over short distances, as do the density, hardness, and grain size. Over longer distances, and over the entire region, there is a surprising amount of convergence in the snow properties. The biggest variations in snow properties are not regional—they are local and associated with topographic breaks and local variations in vegetation.

One clear-cut *within-region* source of variation arises from the presence of lakes. Results from previous SnowSTAR campaigns (Sturm and Liston 2003) and measurements from Daring Lake (currently unpublished) are shown in Table 9. A consistent difference between tundra and lake snow properties is evident from multiple years of data and from sites distributed across North America. SWE on lakes tends to be 63–81% of that measured at tundra sites, while the snow density on lakes ranges from 107 to 126% of that measured on land. As discussed in Sturm and Liston (2003), these differences can be readily explained by processes that operate differently on the tundra than on the lakes. The range of values (Table 9) is

surprisingly narrow, given the generally heterogeneous nature of snow cover: 18% for SWE and 19% for density.

Table 9. Comparison of SnowSTAR 2007 data with previous campaigns.

	Sample Size		Tundra		Lake		Lake-to-Tundra Ratio	
	Tundra	Lakes	SWE (mm)	Density (g/cm <sup>3</sup> )	SWE (mm)	Density (g/cm <sup>3</sup> )	SWE (%)	Density (%)
SnowSTAR 2000	13	13	99	0.285	79	0.344	80	121
SnowSTAR 2002	13	13	94	0.277	68	0.334	72	121
Daring Lake 2004	26	49	126	0.273	97	0.345	77	126
Daring Lake 2005	55	31	95	0.287	75	0.346	79	121
Daring Lake 2006	64	51	137	0.293	102	0.328	74	112
Daring Lake 2007	81	52	117	0.327	74	0.357	63	109
SnowSTAR 2007	14	16	118	0.347	96	0.371	81	107

## Passive Microwave Implications

Ultimately, a traverse like ours is not a practical way to assess the snow conditions across such a broad region. It is too time consuming and labor intensive. Remote sensing of the snow is absolutely essential. A primary reason for the measurements acquired along the traverse was to assist in efforts to develop and validate satellite passive microwave SWE retrieval algorithms specific to open tundra environments. Regional brightness temperature patterns from the Advanced Microwave Scanning Radiometer (AMSR-E) are shown in Figure 17 for the Daring Lake to Baker Lake segment of the traverse. Aside from the oasis of trees along the Thelon River, the domain in Figure 17 is largely north of the treeline. As discussed in the previous section, no strong gradients in snow cover properties were measured. Examination of the HYDRO 1K datasets showed no strong gradients in elevation or topographical complexity along the route of this traverse. In spite of this consistency in snow cover, land cover, and topography, the spatial patterns in the AMSR-E measurements (Fig. 17a to 17d) indicate that the primary influence on the satellite signal appears to be the lake fraction.

The Daring Lake to Baker Lake portion of the traverse route shown in Figure 17 can be broken down into three basic units:

- A lake-rich area in the west composed of a connected sequence of large lakes (i.e. Lac de Gras, Thonokied Lake, Afridi Lake, Aylmer Lake, Clinton-Colden Lake);
- A relatively lake-sparse region that includes the Thelon Oasis; and

- The interconnected large lake system that flows into Chesterfield Inlet at Baker Lake (Beverly Lake, Aberdeen Lake, Schultz Lake to the north, Lake Dubawnt to the south).

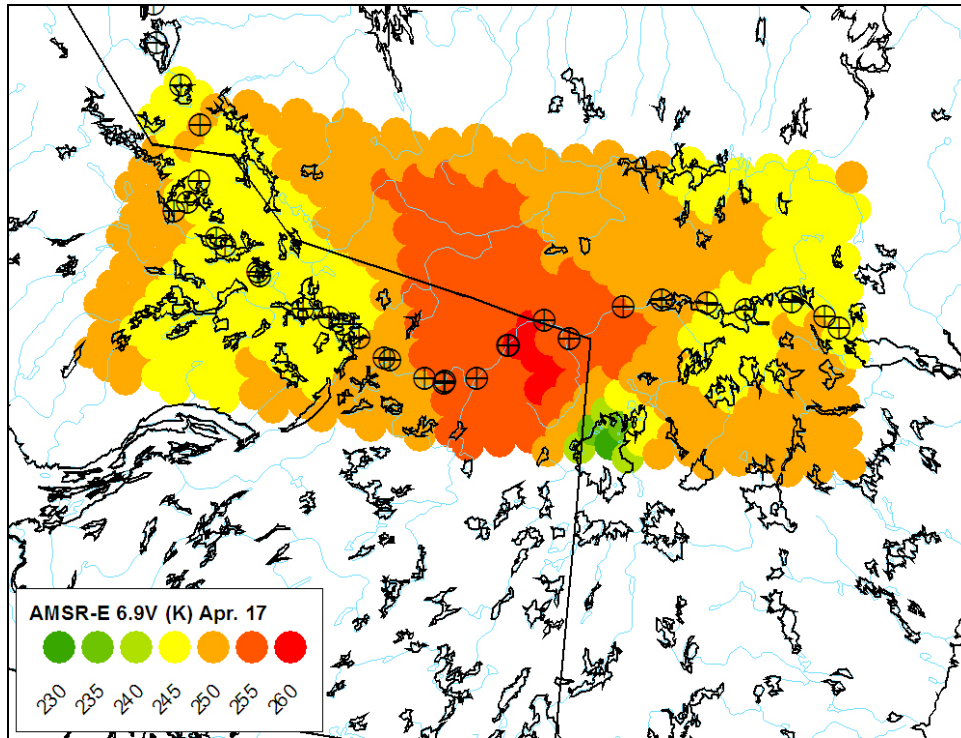
The low-frequency AMSR-E measurements (6.9 and 10.7 GHz) are approximately 5–10 K *lower* across the lake-rich areas (Fig. 17 a and b). The 18.7-GHz measurements exhibit only subtle variations over the region, with a total range of only 5–10 K that is less strongly associated with lake fraction (Fig. 17c). The largest brightness temperature range was observed at 36.5 GHz (Fig. 17d). Unlike the lower frequencies, 36.5-GHz brightness temperatures were up to 30 K *higher* over the two lake-rich portions of the study area.

The sensitivity to the lake fraction is problematic for conventional approaches to retrieving SWE from microwave brightness temperatures. Most SWE retrieval algorithms typically exploit the difference between a measurement frequency sensitive to snow grain volume scatter (~37 GHz) with a measurement frequency considered insensitive to snow (~19 GHz) (Chang et al. 1990, Goodison and Walker 1995, Kelly et al. 2003, Mognard and Josberger 2002, Pulliainen 2006). The larger the difference between these two measurements, the higher the SWE. These particular frequencies are commonly used because they extend continuously through the satellite record (1978 to present). The snow surveys, however, indicated no strong longitudinal gradient in flat tundra and lake SWE across the Daring Lake to Baker Lake portion of the traverse. Lake-rich and lake-poor sections of the traverse had similar mean SWEs because the tundra SWE and lake SWE measurements were quite similar (Table 9). If the SWE exhibited only weak regional variations, and 36.5-GHz measurements are predominantly influenced by the volume scatter of the snowpack, the pattern in Figure 17d should be spatially invariant. Instead, the spatial variability driven by the lake fraction is very clear. To compound the issue, the multi-frequency response to the lake fraction is problematic to the application of brightness temperature difference algorithms. If a high lake fraction increases the 36.5-GHz brightness temperatures by 30 K, but decreases lower-frequency (18.7 or 10.7 GHz) brightness temperatures by only 5–10 K, then higher lake fractions will be systematically associated with lower SWE. This is illustrated in Figure 17e, which shows the AMSR-E 36.5–18.7 brightness temperature difference. Across lake-rich areas, the difference is closer to zero than in lake-poor regions, so the retrieved SWE with a simple brightness temperature

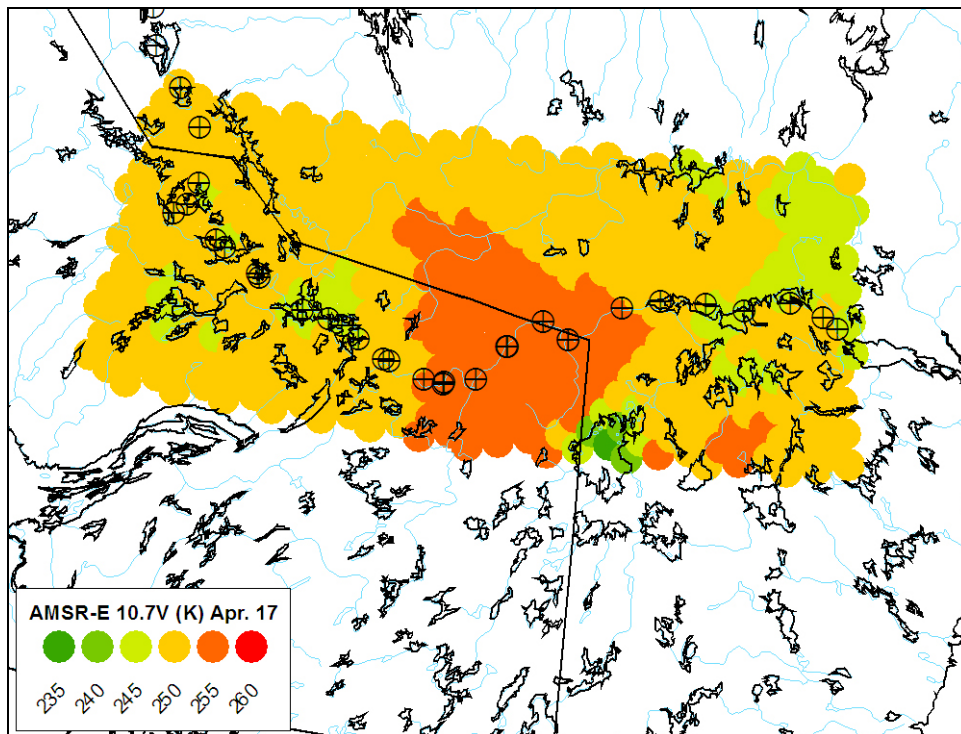
difference algorithm uncorrected for lake fraction would have regional biases unrelated to the snowpack.

Time series of AMSR-E brightness temperatures for a lake-rich (near Lac de Gras) and a lake-poor (near Hoare Lake) grid cell are shown in Figure 18. The time series profiles are similar in shape, with differences between the two grid cells due primarily to brightness temperature magnitude. At the lake-rich site, greater separation of the low-frequency channels is driven by the sensitivity of 6.9 and 10.7 measurements to lake ice cover. The lake fraction influence on the 36.5-GHz brightness temperature magnitude is also clear: the low lake fraction brightness temperatures are approximately 10 K lower and extend across a slightly greater seasonal range than the high lake fraction grid cell. Until early January, there is a substantial period of no change in 36.5-GHz brightness temperature, indicating that a critical depth of snow needs to be reached to produce sufficient volume scatter to alter the signal. The 36.5-GHz measurements reach a minimum in mid-March, even though this is not the end of the snow accumulation season and air temperatures remain cold. By this point, brightness temperatures no longer decrease with increasing SWE but actually start to increase, a phenomenon related to the relative scattering influence of grain size in a deepening snowpack and observed in other locations under deep snow conditions (De Seve et al. 1997, Matzler 1994).



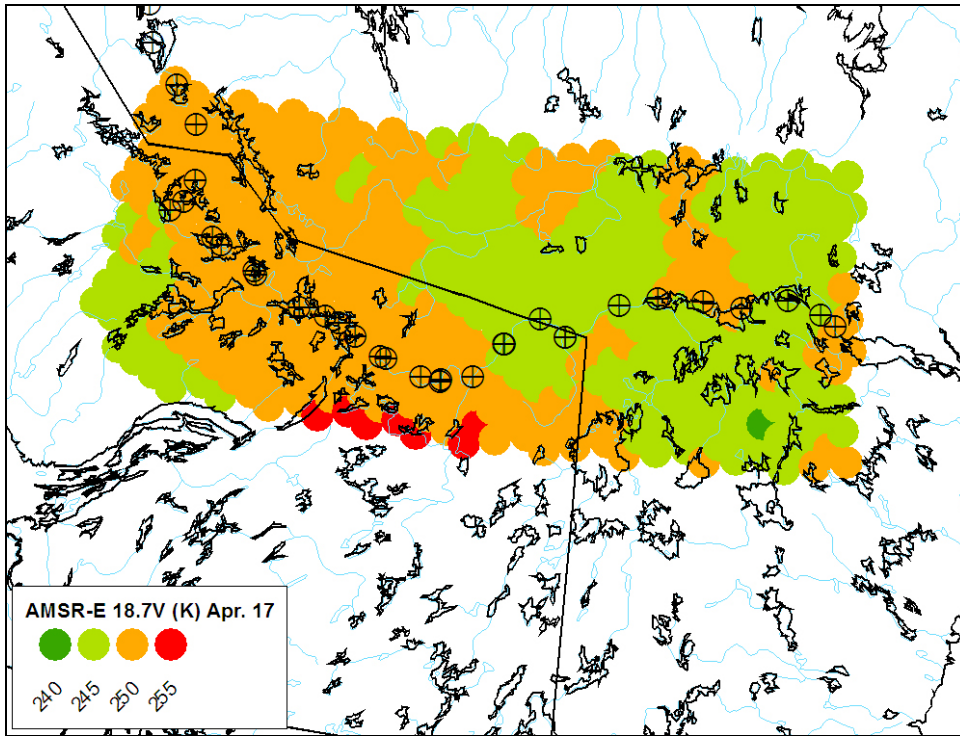


a. 6.9 GHz.

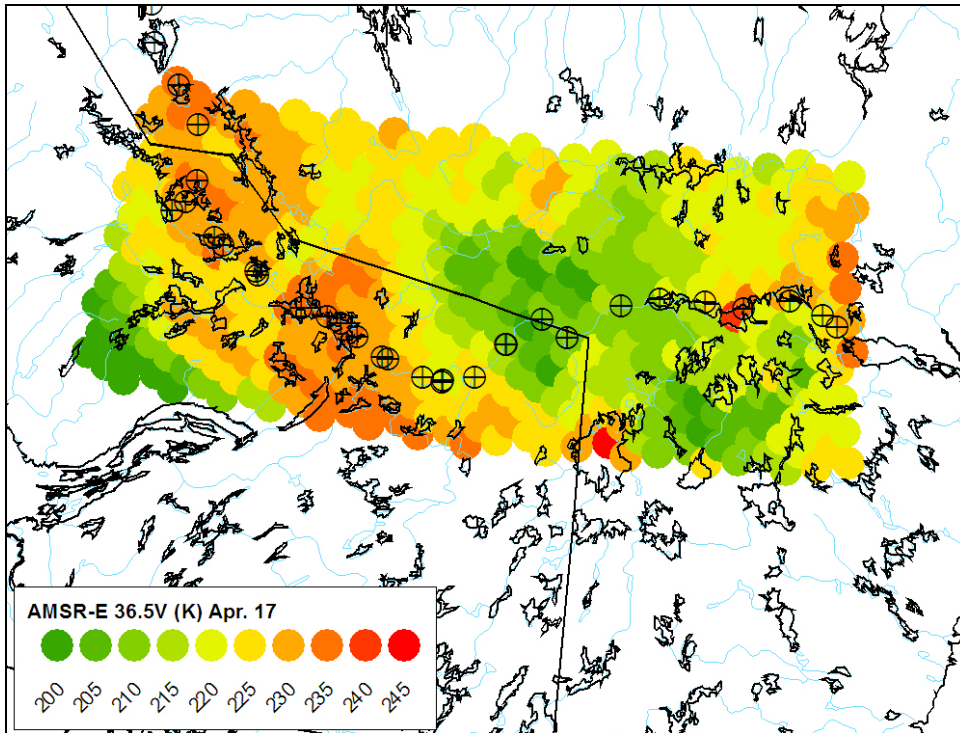


b. 10.7 GHz.

Figure 17. Vertically polarized AMSR-E brightness temperatures for April 17. Symbols denote sample site locations.

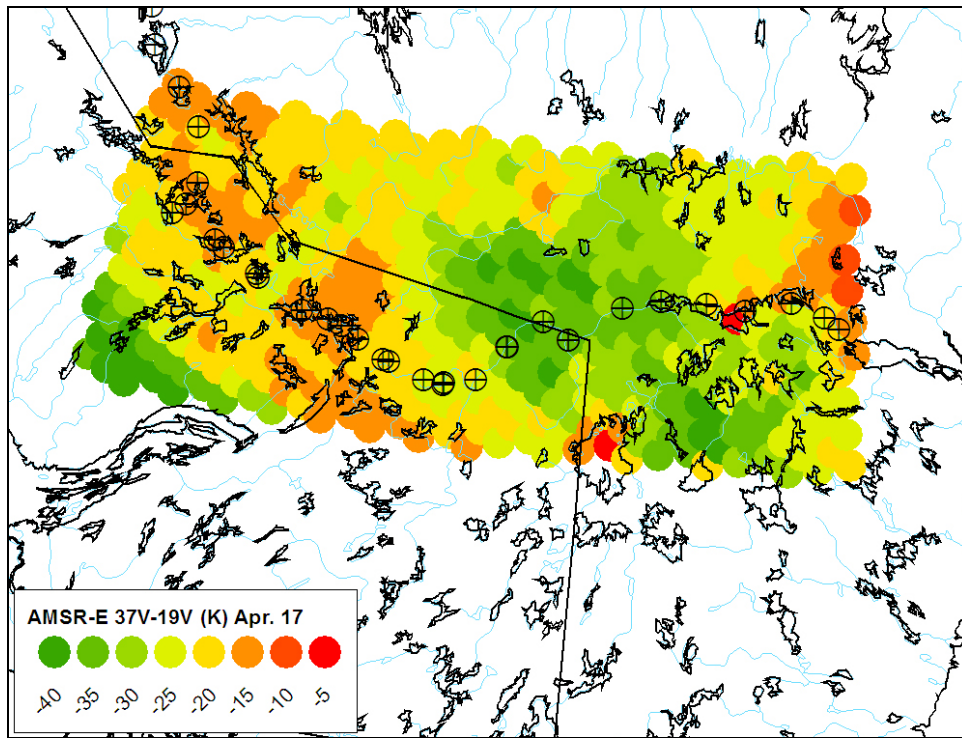


c. 18.7 GHz.

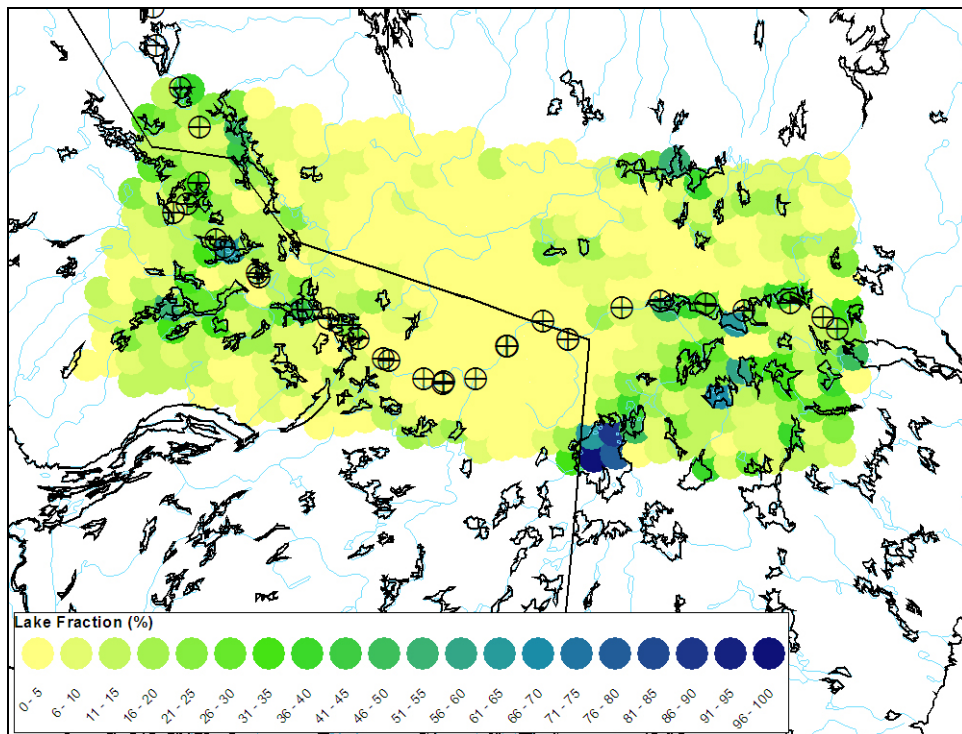


d. 36.5 GHz.

Figure 17 (cont.). Vertically polarized AMSR-E brightness temperatures for April 17.



e. 36.5-18.7.



f. Lake fraction estimates from the USGS in the EASE-Grid.

Figure 17 (cont.). Vertically polarized AMSR-E brightness temperatures for April 17.

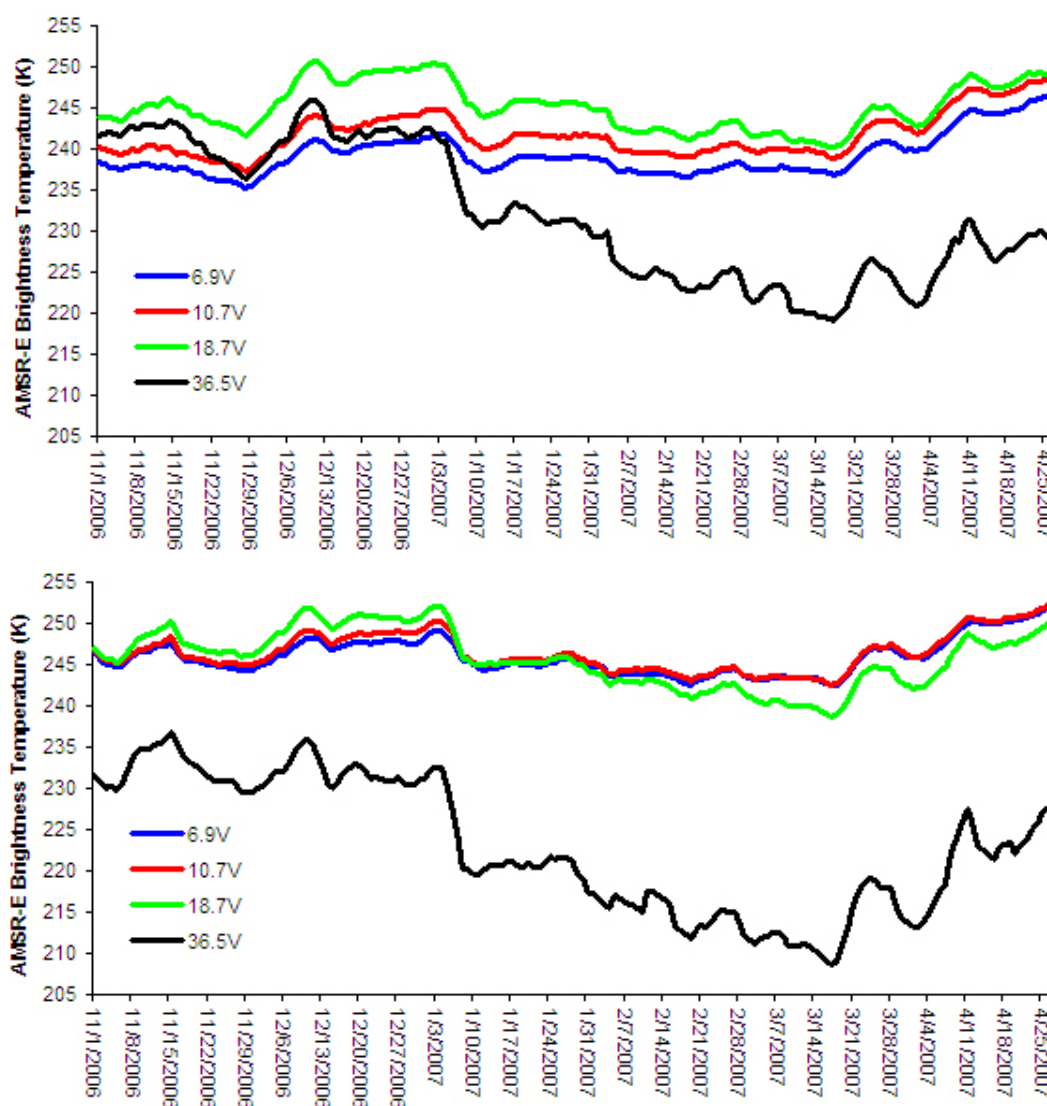


Figure 18. AMSR-E brightness temperature time series for lake-rich (top) and lake-poor (bottom) grid cells.

The choice of polarization is not consistent among microwave SWE algorithms: some utilize horizontal measurements (Chang et al. 1990, and the modified versions of Foster et al. 1997, Kelly et al. 2003), while others are based on vertical measurements (Goodison and Walker 1995, Mognard and Josberger 2002, Goita et al. 2003, Pulliainen 2006). One advantage of vertical polarization measurements is the reduced sensitivity to ice lenses within the snowpack. An opportunity to assess this sensitivity arose because of the rain-on-snow event in the vicinity of Daring Lake on 7 April 2007. The 36.5-GHz polarization gradient (V-H) was calculated for 3 April 2007 (pre-event, cold conditions) and 9 April 2007 (post-event, cold conditions). The difference between these two dates is illustrated in Figure 19. No difference is evident over the majority of the study area, except in

the region of Daring Lake (and west) where the difference in polarization gradient between the two dates reaches 30 K. This difference is driven by a strong response in the horizontal polarization measurements (not shown). The extent of the polarization gradient difference agrees well with observations of a surface ice layer (0.1–0.5 cm thick) at sites extending from north of Yamba Lake, south to Lake Providence, and east to Thonokied Lake (as noted in Fig. 19).

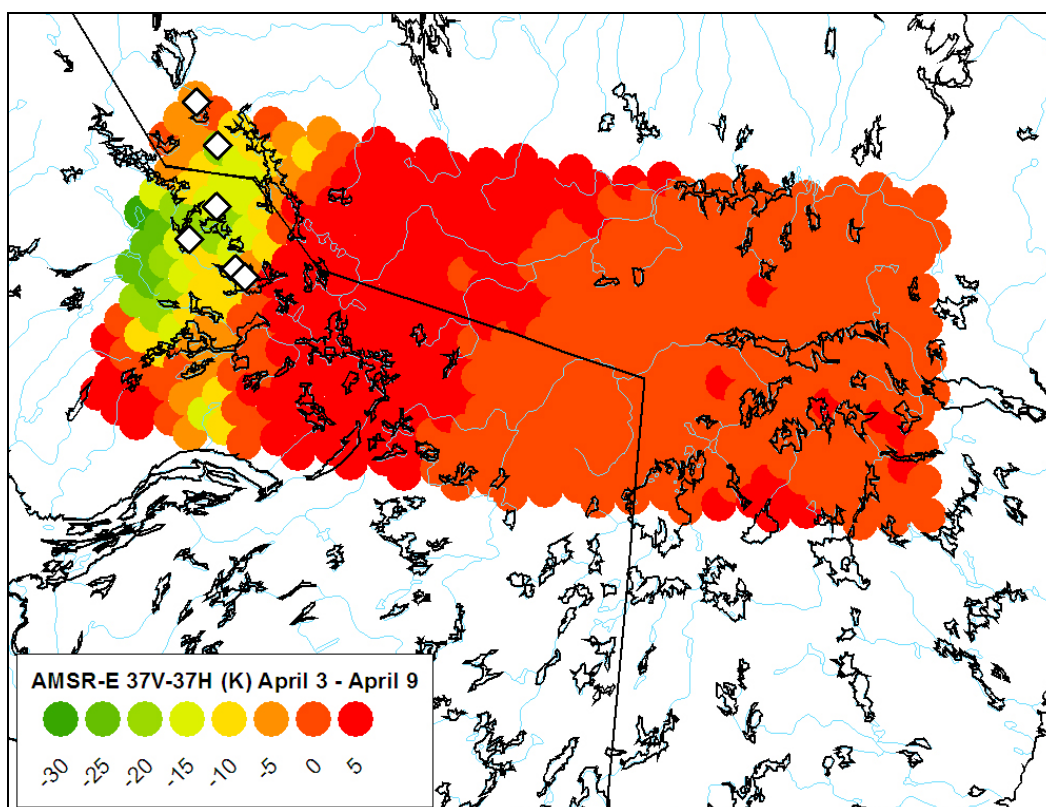


Figure 19. AMSR-E 36.5-GHz polarization gradient (V-H) for April 3 versus April 9 (pre- and post- rain-on-snow event). Symbols denote measurements sites with a surface ice layer.

Given the impact of the sub-grid-scale lake fraction on passive microwave brightness temperatures, the measurements from Great Bear Lake provided an opportunity to examine AMSR-E footprints composed completely of lake ice. We hoped this would allow separation of the snow vs. ice signal. Great Bear Lake was sampled from the southwest (near the community of Deline) to the northeast (towards the Dease Arm) between April 2 and 4, 2007. A general trend of deeper and less dense snow in the south to shallower but more dense snow in the north was identified (Table 10). More clearly defined was the relationship between snow depth and ice thickness: deeper (shallower) snow was associated with thinner (thicker)

ice (Fig. 20). The slope of the snow depth/ice thickness relationship across Great Bear Lake was consistent with other lakes sampled on the traverse (Fig. 20), although the ice was generally thinner, probably due to typically later freeze-up.

Table 10. Summary of measurements across Great Bear Lake (see Fig. 21 for site locations). GBL1 to GBL5 define a line running southwest to northeast.

Site	Depth (cm)	SWE (mm)	Density (g/cm <sup>3</sup> )	Ice Thickness (cm)
GBL1	25.7	82.0	0.318	124
GBL2	34.1	92.4	0.270	83
GBL3	21.7	74.7	0.342	108
GBL4	23.2	86.2	0.369	137
GBL5	15.3	61.9	0.397	151

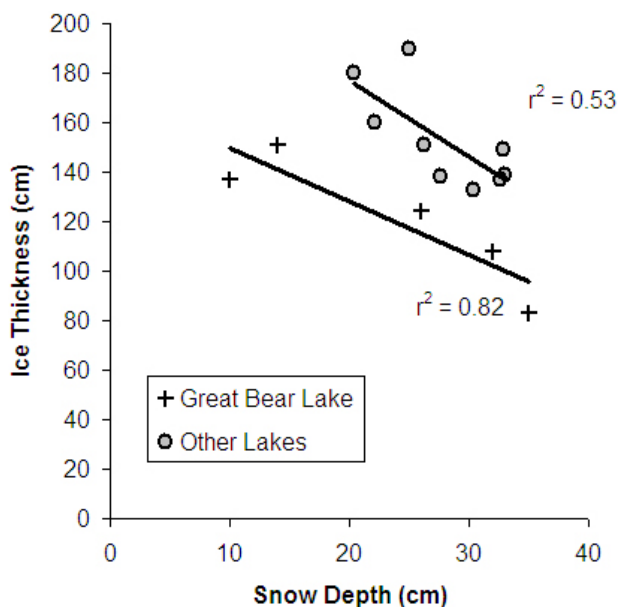
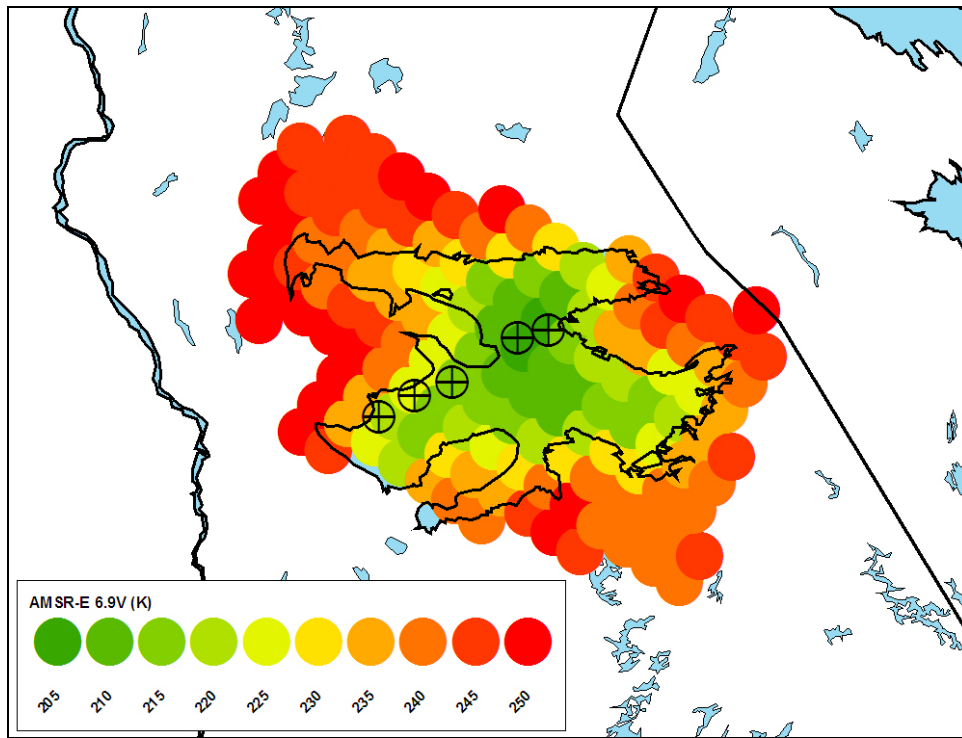


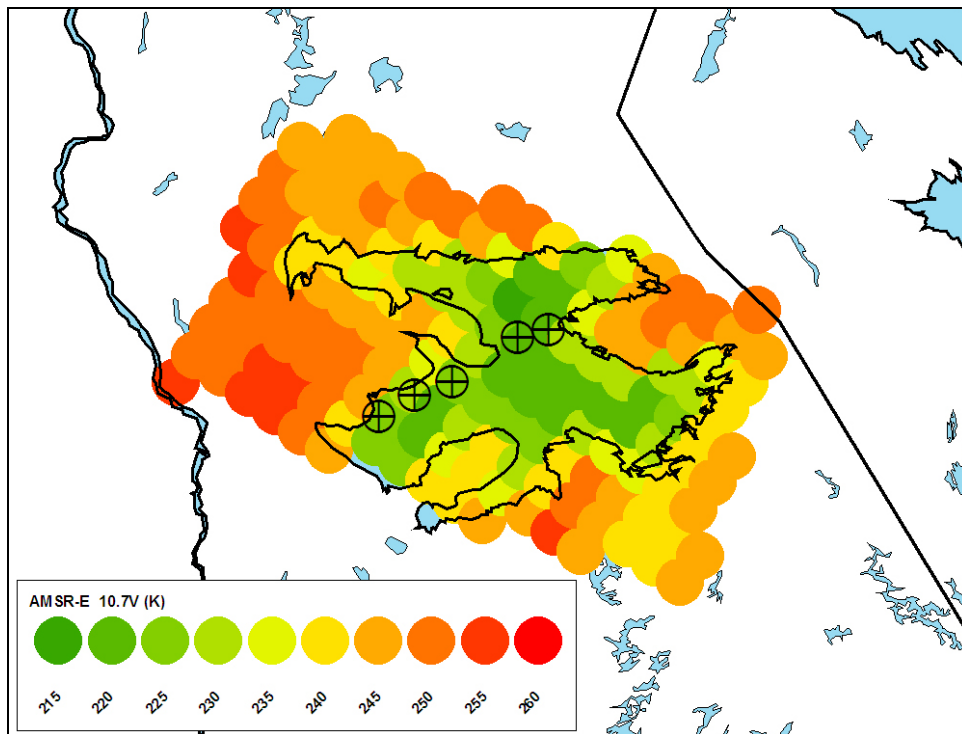
Figure 20. Relationships between snow depth and ice thickness.

Patterns of AMSR-E brightness temperatures across Great Bear Lake are shown in Figure 21a-d. A summary of the brightness temperature ranges observed over homogeneous lake and terrestrial footprints is provided in Table 11. The microwave signature for homogeneous lake ice is 30–50 K lower than the signature for terrestrial areas for 6.9 and 10.7 GHz and 20–50 K higher for 36.5 GHz. These are the frequencies where the contrast between lake and land are greatest. In many ways, the contrast is the same as discussed previously between areas of high and low lake fractions,

though (not surprisingly) the contrast is enhanced when comparing “pure” ice signals to “pure” land signals. The 36.5–18.7-GHz brightness temperature difference is near zero across most of the lake (Fig. 21e). SWE retrievals based on conventional algorithms (which assume that this difference is proportional to the snow cover) would fail, as has been discussed by Duguay et al. (2005) and Green (2006). In short, the lake signal dominates the results, with any gradients in the snowpack virtually invisible.



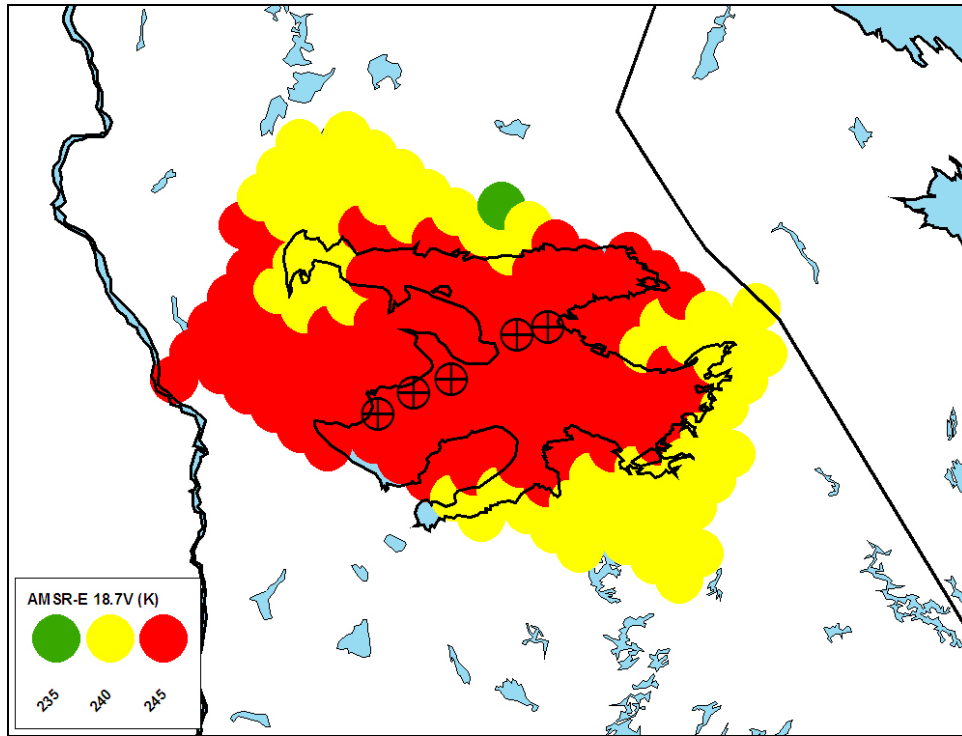
a. 6.9 GHz.



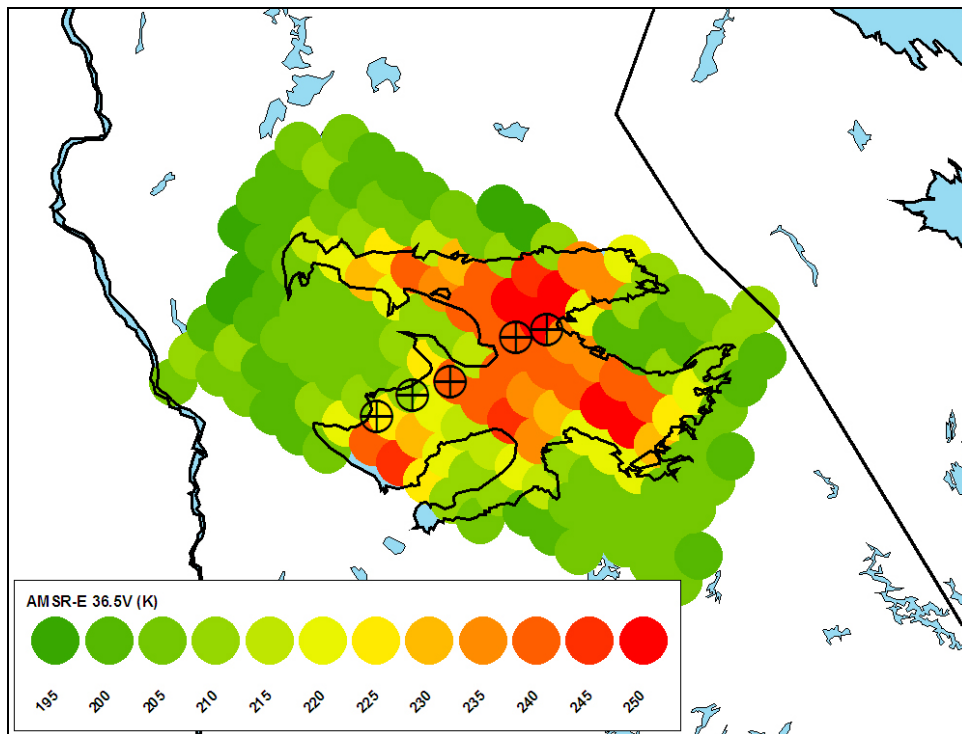
b. 10.7 GHz.

Figure 21. Vertically polarized AMSR-E brightness temperatures for April 3.



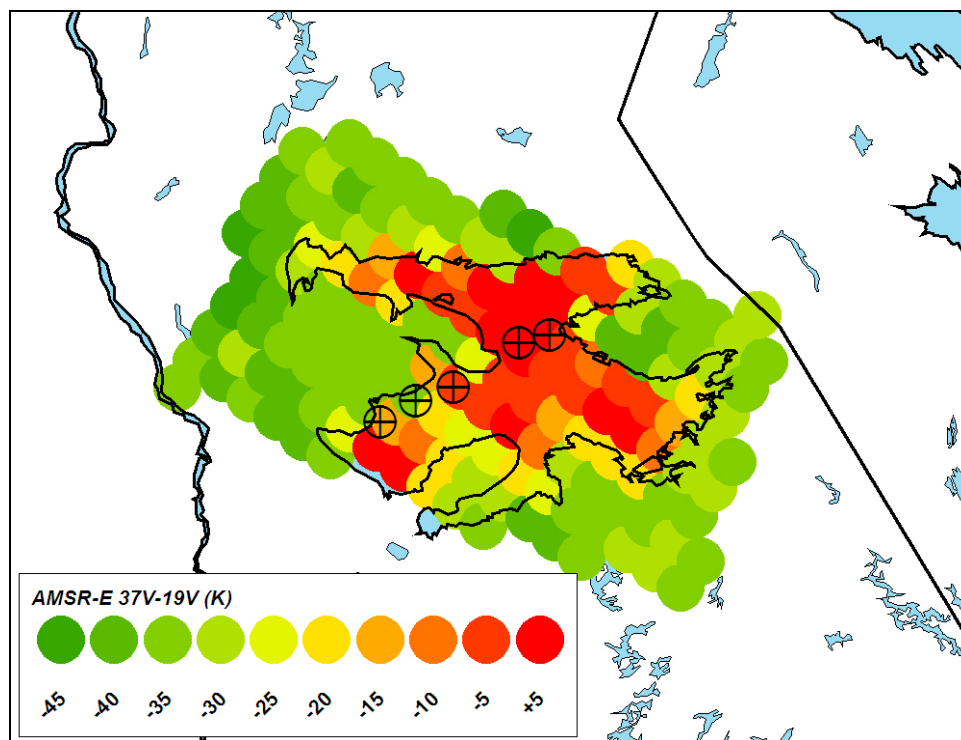


c. 18.7 GHz.



d. 36.5 GHz.

Figure 21 (cont.). Vertically polarized AMSR-E brightness temperatures for April 3.



e. 36.5– 18.7.

Figure 21 (cont.). Vertically polarized AMSR-E brightness temperatures for April 3.

Table 11. AMSR-E Brightness temperature ranges for the Great Bear Lake region.

Frequency	Brightness Temperature Range (K)		
	All	Terrestrial	Lake
6.9V	50 (204-254)	10 (240-250)	22 (204-226)
10.7V	37 (214-251)	14 (234-248)	16 (214-230)
18.7V	11 (234-245)	6 (234-240)	4 (240-244)
36.5V	56 (191-247)	14 (191-205)	35 (210-245)

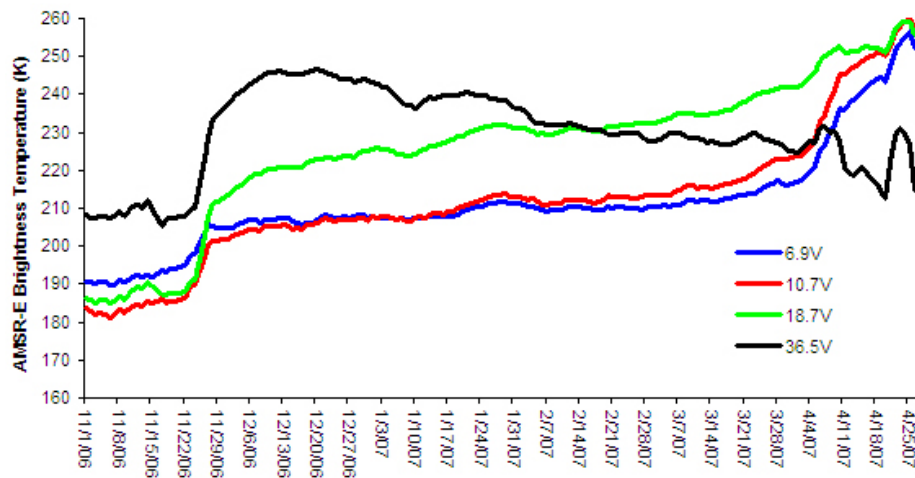
Looking only at the data from Great Bear Lake, a correlation analysis between the AMSR-E data and the surface measurements indicated that increasing snow depth produced higher values of brightness temperature at the lower frequencies and lower brightness temperature values for the higher frequencies. Increasing ice thickness produced the exact opposite effect (Table 12). The linkage between the effect of snow and ice was expected, given the correlation between these two variables (Fig. 20). These results are somewhat unexpected. Airborne measurements described in Hall et al. (1981) showed a correlation in the opposite direction: thinner ice was associated with lower brightness temperatures

at low frequencies. At 36.5 GHz, we found deeper snow (thinner ice) to be associated with lower brightness temperatures.

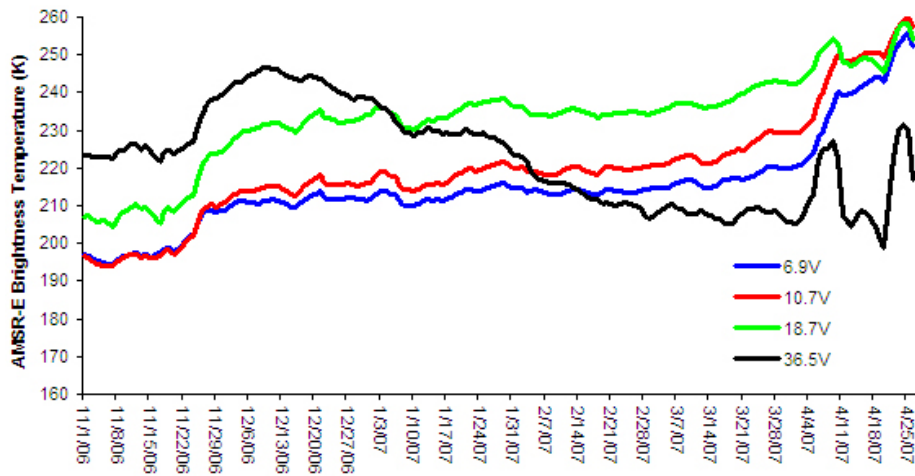
Table 12. Regression results for coincident AMSR-E brightness temperatures and surface measurements of snow depth and ice thickness.

	6.9V (K)	10.7V (K)	18.7V (K)	36.5V (K)	37-19 Crossover (DOY)
Snow Depth	0.91	0.93	-0.31	-0.73	-0.78
Ice Thickness	-0.86	-0.96	0.40	0.86	0.90

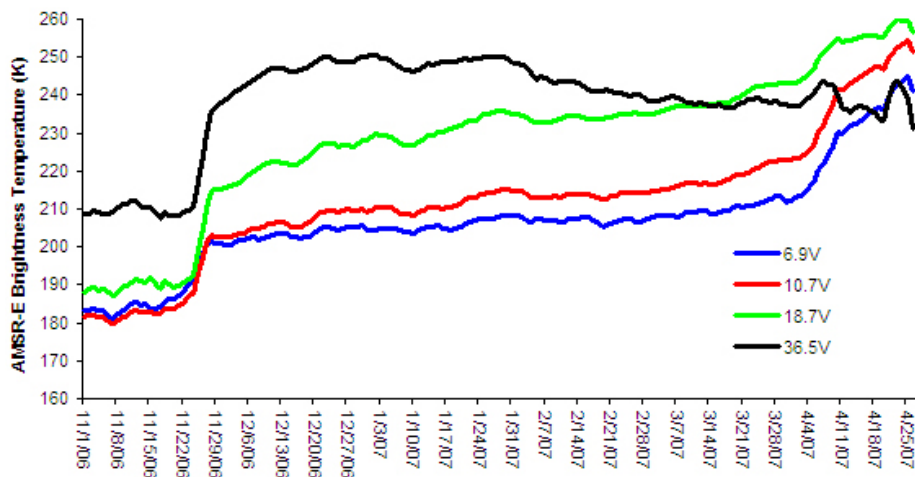
Time series of AMSR-E brightness temperatures at the Great Bear Lake surface measurement sites for the complete winter season are shown in Figure 22. The freeze-up timing in mid-November is clearly identified by a sharp increase in brightness temperatures at all frequencies. A subtle upward drift in 6.9, 10.7, and 18.7 GHz measurements, likely due to increasing ice thickness, occurs until melt onset, at which time brightness temperatures rise sharply again. The 36.5-GHz measurements decrease through the ice-covered season, but unlike at terrestrial sites, they do not fall below the 18.7-GHz signals early in the snow cover season. Instead, this crossover point ( $36.5 < 18.7$  GHz) occurs progressively later in the season as one goes northward (mid-February at site GBL1; early April at site GBL5). The historic literature (Douglas 1914) talks about the climate north of Great Bear Lake being considerably colder than along the southern margin of the lake. The later cross-over date (and thicker ice in the north) may reflect this climatic difference as expressed through the properties of the lake ice and overlying snow cover.



a. Great Bear Lake Site 1.

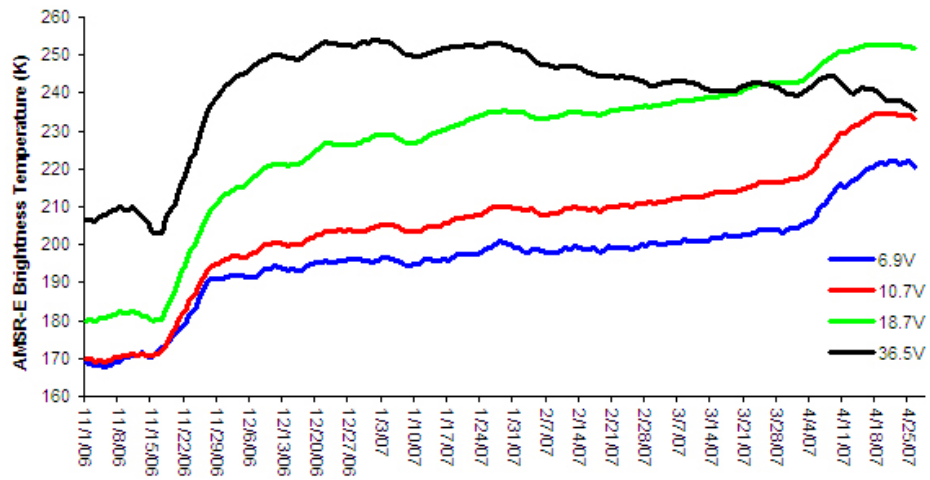


b. Great Bear Lake Site 2.

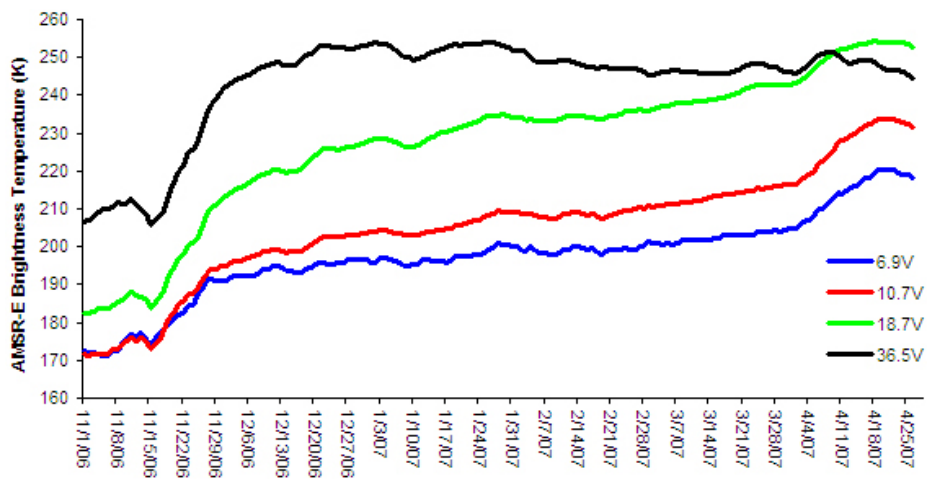


c. Great Bear Lake Site 3.

Figure 22. AMSR-E brightness temperature time series for the Great Bear Lake surface measurement sites.



d. Great Bear Lake Site 4.



e. Great Bear Lake Site 5.

Figure 22 (cont.). AMSR-E brightness temperature time series for the Great Bear Lake surface measurement sites.

## 5 Discussion

Most snow studies are local in nature. It takes a substantial amount of time, effort, and money to collect a comprehensive set of snow measurements at a continental scale. But is collecting such a set valuable? The answer depends on whether the data collected are representative or biased. Collecting data at this large scale can be discouraging because it is easy to see how much of the complexity of the snow cover on the landscape is being ignored. By necessity, one has to drive past many kilometers of snow before stopping at a measurement station. Is that station typical of the snow one has just passed by? Does the necessity of traveling where there is a trail or a lake bias the selection of sample points? There is a constant tension between traveling (there are always time constraints on such a sample campaign) and stopping to make measurements. Despite these issues, the data collected in 2007 show surprisingly consistent patterns, suggesting that the sampling bias was not too severe and that while local variations did exist, regional variations were captured. In addition, working at the continental scale forced us to think broadly about the snow cover, and this is a valuable perspective for climate studies and remote sensing applications.

At the broadest scale, the results validate the idea we put forward in 1995 (Sturm et al. 1995) that there was a distinct class of snow called tundra snow. In general, the snow properties we observed on the traverse were clustered within narrow limits of depth, density, and grain/layer characteristics, and these were similar to the range of properties we had observed farther west in Alaska and farther south in Manitoba. As we discussed previously, the new results, combined with the old, indicate that the tundra snow class stretches over 6000 km across arctic and sub-arctic North America. It is likely that within that band, there are regional differences in the amount of wind slab and depth hoar, but overall, these are second-order effects.

The results also confirm that if we want to use remote sensing to monitor tundra snow, we must deal with the problem of lakes. In particular, our results from Great Bear Lake confirm that when the lake fraction is high, snow cover properties cannot be determined by the current generation of passive microwave sensors and algorithms. It is possible that clever use of

multiple frequencies and polarizations will allow better microwave retrievals in lake-rich country, and research to that end is needed, but it seems likely that multisensor (optical, radar, and passive microwave) techniques, as well as inferential methods and modeling, will be needed to solve this problem.

Lastly, we were able to demonstrate on the traverse that near-infrared photography can be used effectively to document snowpit stratigraphy. Matzl and Schneebeli (2007) showed that the method had promise in this respect, but they did not address how robust or efficient the method might be. The results (Appendix B) speak for themselves: we were able to document stratigraphy rapidly and efficiently in conditions that were often less than favorable. We believe the method should become a standard snowpit practice.

The area of the traverse is a part of the Arctic that is warming rapidly. One ramification of the warming is likely to be a change in the winter snow cover. Unfortunately, we have not found any descriptions of the snow cover against which we can compare our 2007 results. Most travelers across the region were either struggling to stay alive, looking for gold or diamonds, or touring. Our results may be useful in 25 years as a baseline against which present conditions can be compared. We might speculate on several changes in snow characteristics. Rain-on-snow and winter thaw events may become more common. This would lead to more ice layers such as the one we observed at and east of Daring Lake. These layers have implications for wildlife and would clearly complicate remote sensing. Depth hoar percentages might go down, while wind slab percentages go up. Warmer winters would produce less metamorphism, so fewer slabs would be converted into depth hoar. Paradoxically, because slabs have a higher thermal conductivity than depth hoar (Sturm et al. 1997), this might actually lead to lower winter soil temperatures, which has ecosystem impacts.

## 6 Conclusion

Detailed snow measurements made during a 4200-km route from Alaska through Northwest Territories and Nunavut, Canada, in April 2007 show that tundra snow covers much of the region. This snow cover consists of depth hoar and wind slab with small and ephemeral fractions of new, recent, and icy snow. The snow tends to be shallow (<40 cm deep) with less than six layers. Where deposited on lake and river ice, the snow is shallower, denser, and more metamorphosed than where deposited on tundra. Lakes and lake ice confound passive microwave remotes sensing of the snow cover in this area because the lake signal overwhelms the snow signal. Consequently, challenges remain in developing methods to monitor this snow cover by satellite. The traverse, however, demonstrated the practicality of making measurements across the area that can be used to improve remote monitoring methods and that can also provide baseline data against which future changes in snow cover due to climate change can be compared.



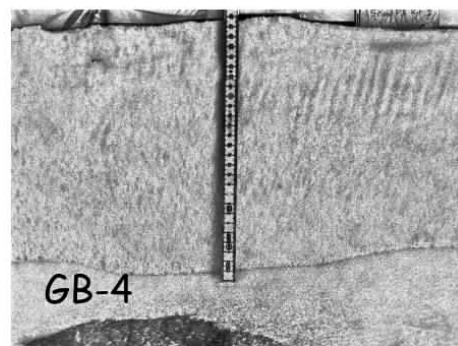
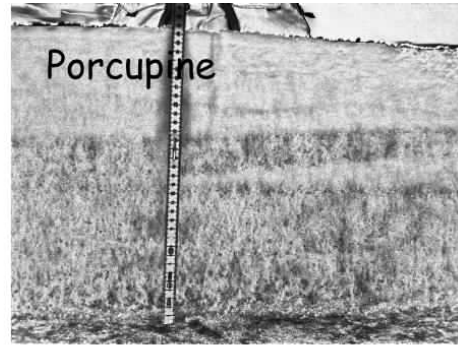
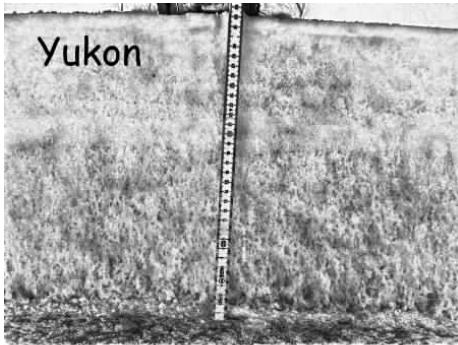
## References

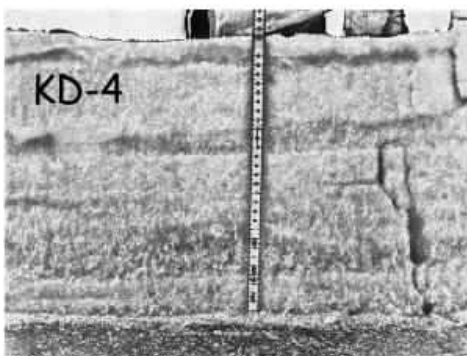
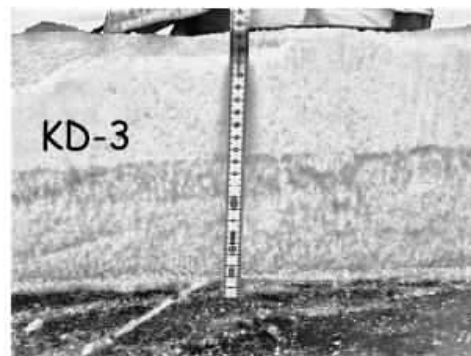
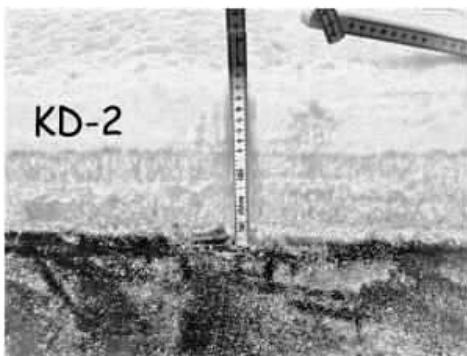
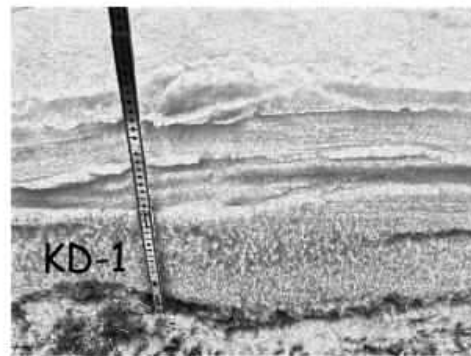
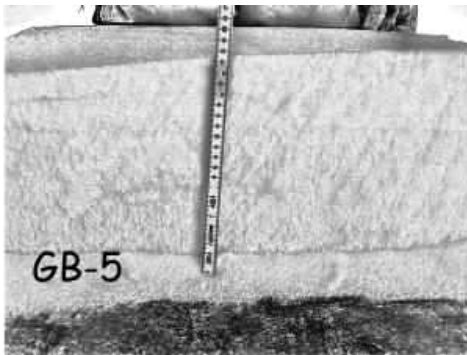
- Benson, C.S. 1969. *The Seasonal Snow Cover of Arctic Alaska*. Calgary, Alberta, Canada: The Arctic Institute of North America.
- Benson, C.S., and M. Sturm. 1993. Structure and wind transport of seasonal snow on the Arctic slope of Alaska. *Annals of Glaciology* 18: 261–267.
- Chang, A., J. Foster, and D. Hall. 1990. Satellite sensor estimates of northern hemisphere snow volume. *International Journal of Remote Sensing* 11(1): 167–171.
- Colbeck, S., E. Akitaya, R. Armstrong, H. Gubler, J. Lafeuille, K. Lied, D. McClung, and E. Morris. 1992. *The International Classification for Seasonal Snow on the Ground*. Hanover, NH: The International Commission on Snow and Ice of the International Association of Scientific Hydrology/International Glaciological Society/U.S. Army CRREL.
- De Seve, D., M. Bernier, J.-P. Fortin, and A. Walker. 1997. Preliminary analysis of snow microwave radiometry using the SSM/I passive-microwave data: The case of La Grande River watershed (Quebec). *Annals of Glaciology* 25: 353–361.
- Derksen, C., A. Walker, and B. Goodison. 2003. A comparison of 18 winter seasons of in situ and passive microwave-derived snow water equivalent estimates in Western Canada. *Remote Sensing of the Environment* 88: 271–282.
- Derksen, C., A. Walker, and B. Goodison. 2005. Evaluation of passive microwave snow water equivalent retrievals across the boreal forest/tundra transition of western Canada. *Remote Sensing of the Environment* 96(3/4): 315–327.
- Douglas, G.M. 1914. *Lands Forlorn*. New York: G. P. Putnam's Sons.
- Douglas, T.A., and M. Sturm. 2004. Arctic Haze, mercury and the chemical composition of snow across northwestern Alaska. *Atmospheric Environment* 38(2004): 805–820.
- Duguay, C., J. Green, C. Derksen, M. English, A. Rees, M. Sturm, and A. Walker. 2005. Preliminary assessment of the impact of lakes on passive microwave snow retrieval algorithms in the Arctic. *Proceedings, 62nd Eastern Snow Conference, Waterloo, Ontario*. 223–228.
- Foster, J., A. Chang, and D. Hall. 1997. Comparison of snow mass estimates from a prototype passive microwave snow algorithm, a revised algorithm and a snow depth climatology. *Remote Sensing of the Environment* 62: 132–142.
- Goita, K., A. Walker, and B. Goodison. 2003. Algorithm development for the estimation of snow water equivalent in the boreal forest using passive microwave data. *International Journal of Remote Sensing* 24(5): 1097–1102.

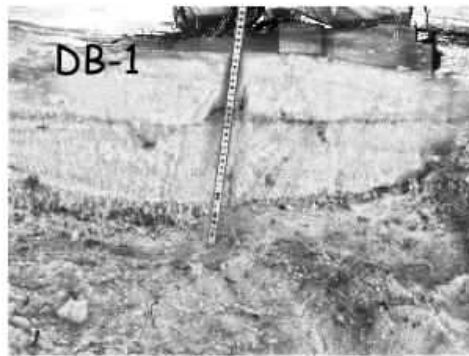
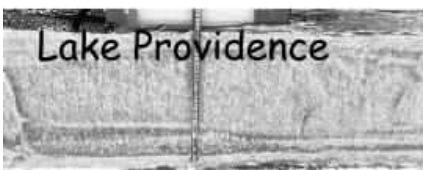
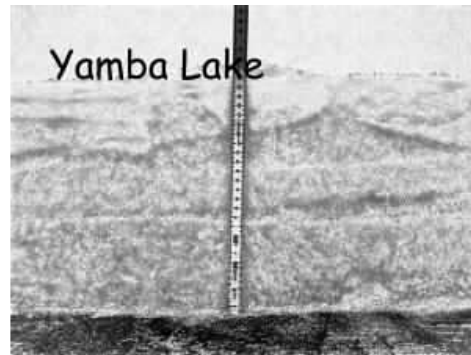
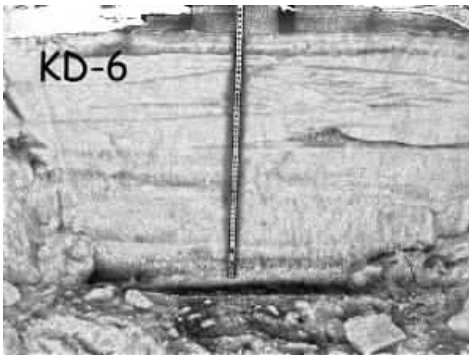
- Goodison, B., and A. Walker. 1995. Canadian development and use of snow cover information from passive microwave satellite data. In *Passive Microwave Remote Sensing of Land-Atmosphere Interactions*. ed. B. Choudhury, Y. Kerr, E. Njoku, and P. Pampaloni. 245–262. Utrecht, Netherlands: VSP BV.
- Granberg, H. 1978. Snow accumulation and roughness changes through winter at a forest-tundra site near Schefferville-Quebec. In *Proceedings, Modeling of Snow Cover Runoff*. ed. S.C. Colbeck and M. Ray. 38–92. Hanover, NH: U.S. Army Cold Regions Research and Engineering Laboratory.
- Green, J. 2006. Assessing the impact of sub-grid lakes on SWE estimations—North Slope, Alaska, USA. M.S. Thesis. Fairbanks, AK: University of Alaska Fairbanks.
- Hall, D., J. Foster, A. Chang, and A. Rango. 1981. Freshwater ice thickness observations using passive microwave sensors. *IEEE Transactions on Geoscience and Remote Sensing* GE19(4): 189–193.
- Kelly, R., A. Chang, L. Tsang, and J. Foster. 2003. A prototype AMSR-E global snow area and snow depth algorithm. *IEEE Transactions on Geoscience and Remote Sensing* 41(2): 230–242.
- Liston, G.E., and M. Sturm. 2002. Winter precipitation patterns in arctic Alaska determined from a blowing snow model and snow depth observations. *Journal of Hydrometeorology* 3(5): 646–659.
- Matzl, M. and M. Schneebeli. 2007. Measuring the specific surface area of snow by near-infrared photography. *Journal of Glaciology* 52(179): 558–564.
- Matzler, C. 1994. Passive microwave signatures of landscapes in winter. *Meteorology and Atmospheric Physics* 54: 241–260.
- Mognard, N., and E. Josberger. 2002. Seasonal evolution of snowpack parameters, northern Great Plains. *Annals of Glaciology* 34: 15–23.
- Olsson, P.Q., L.D. Hinzman, M. Sturm, G.E. Liston, and D.K. Kane. 2002. *Surface climate and snow-weather relationships of the Kuparuk Basin on Alaska's Arctic Slope*. ERDC/CRREL TR-02-10. Hanover, NH: U.S. Army Engineer Research and Development Center, Cold Regions Research and Engineering Laboratory.
- Pulliaainen, J. 2006. Mapping of snow water equivalent and snow depth in boreal and sub-arctic zones by assimilating spaceborne microwave radiometer data and ground-based observations. *Remote Sensing of the Environment* 101(2): 257–269
- Rees, A., C. Derksen, M. English, A. Walker, and C. Duguay. 2006. Uncertainty in snow mass retrievals from satellite passive microwave data in lake-rich high-latitude environments. *Hydrological Processes* 20: 1019–1022.
- Sturm, M., and C.S. Benson. 2004. Scales of spatial heterogeneity for perennial and seasonal snow layers. *Annals of Glaciology* 38: 253–260.
- Sturm, M., and G.E. Liston. 2003. The snow cover on lakes of the Arctic Coastal Plain of Alaska. *Journal of Glaciology* 49(166): 370–380.

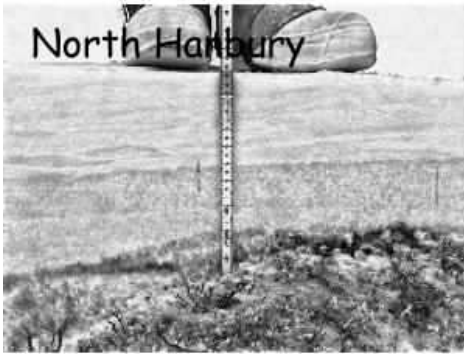
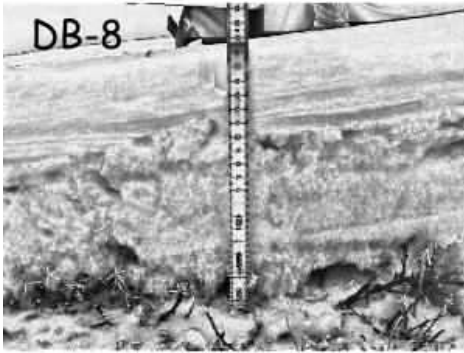
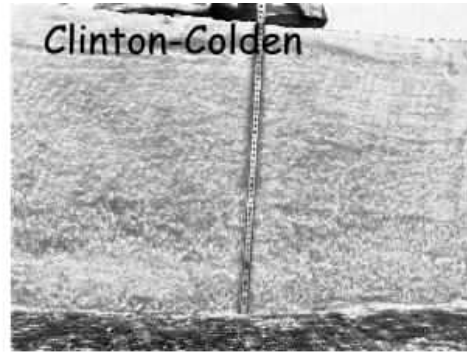
- Sturm, M., J. Holmgren, and G. Liston. 1995. A seasonal snow cover classification system for local to global applications. *Journal of Climate* 8: 1261–1283.
- Sturm, M., J. Holmgren, M. König, and K. Morris. 1997. The thermal conductivity of seasonal snow. *Journal of Glaciology* 43(143): 26-41.
- Sturm, M., J. Johnson, and J. Holmgren. 2004. Variations in the mechanical properties of arctic and subarctic snow at local (1-m) to regional scales (100-km). In *Proceedings of the International Symposium on Snow Monitoring and Avalanches, 12-16 April 2004, Manali, India*. SASE, 233-244.
- Sturm, M., B. Taras, C. Derksen, G.E. Liston, T. Jonas, and J. Lea. In review. Converting snow depth to snow water equivalent using bulk density estimates. *Water Resources Research*.
- Taras, B., M. Sturm, and G.E. Liston. 2002. Snow-ground interface temperatures in the Kuparuk River Basin, Arctic Alaska, U.S.A.: Measurements and Model. *Journal of Hydrometeorology* 3(4): 377-394.
- Tyrrell, J. W. 1897. *Across the Subarctics of Canada: A Journey of 3200 Miles by Canoe and Snowshoe through the Barren Lands*. Toronto, Ontario, Canada: William Briggs.

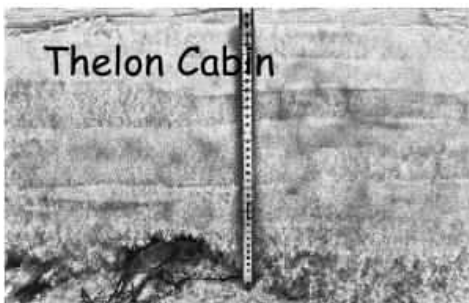
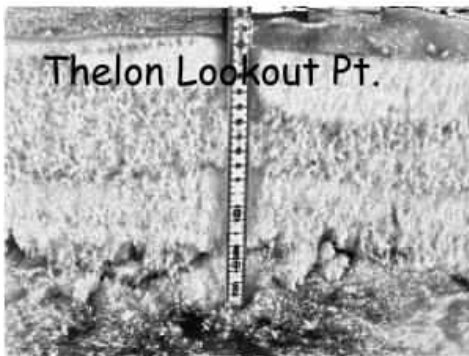
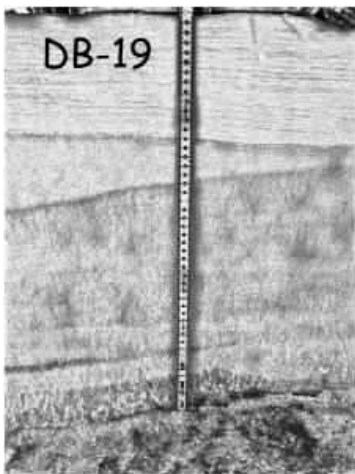
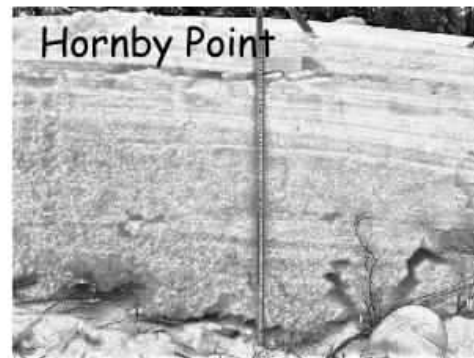
# Appendix A: NIR Images



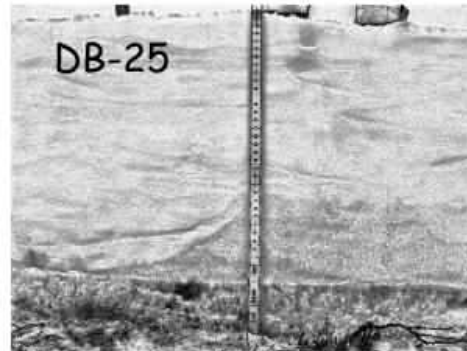
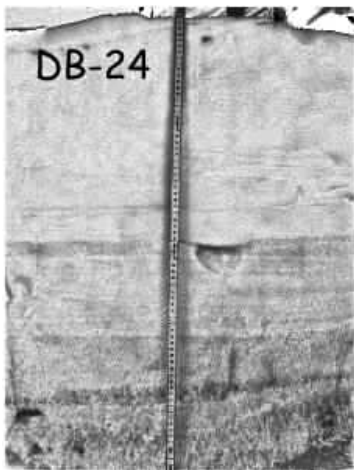
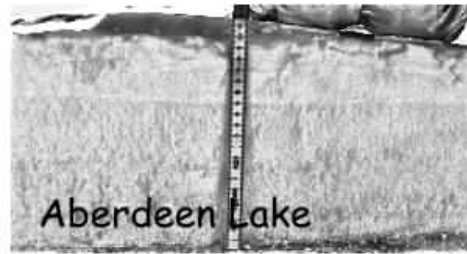
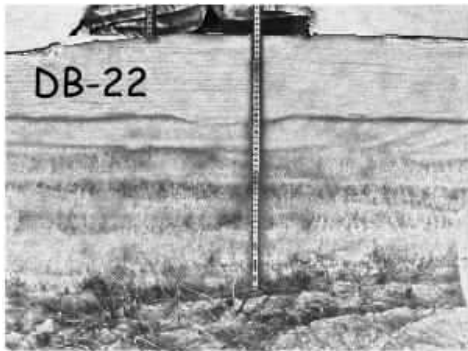


































DB24	DB24	DB24	DB24	DB24	DB24	DB25	DB25	DB25	DB25	DB25	DB26	DB26	DB26	DB26	DB26
72.4	69.7	30.3	46.1	16.5	57.1	53.7	53.9	47.5	57.0	57.4	32.1	36.9	47.5	47.6	30.8
76.6	61.6	29.4	50.3	8.6	41.6	59.2	45.4	37.2	46.5	45.7	35.2	22.4	38.6	46.4	24.3
74.2	60.0	26.6	55.9	9.1	47.6	51.5	43.0	52.2	43.4	45.4	26.7	37.8	46.8	49.6	24.5
75.4	63.7	29.9	41.3	9.1	41.0	53.2	32.9	48.1	45.1	40.7	32.6	32.0	45.5	41.1	28.9
66.3	54.2	25.1	42.4	34.8	47.0	45.1	34.0	50.5	38.9	43.7	29.9	30.8	42.6	44.7	27.0
74.2	59.4	26.7	40.0	33.8	61.3	46.8	25.7	60.7	32.3	57.8	30.3	33.5	46.1	44.2	37.5
75.7	60.7	26.1	26.2	51.4	30.6	41.6	32.3	58.6	36.0		35.4	28.5	47.5	52.2	30.8
79.8	56.7	28.0	37.2	76.8	50.1	41.2	41.6	59.8	35.9		23.0	30.1	49.9	49.2	33.9
72.6	39.3	21.5	11.0	35.1	45.6	44.9	38.7	57.4	38.1		30.6	32.1	47.2	51.2	30.0
71.9	62.7	28.7	12.0	61.6	48.7	42.4	34.3	57.6	37.2		31.0	28.4	48.2	53.6	33.8
70.3	65.1	32.7	12.5	60.2	43.2	48.0	27.4	56.3	41.8		26.7	23.0	46.2	42.5	36.0
76.7	60.1	33.2	39.8	57.2	59.3	36.4	27.4	60.6	41.3		25.1	19.6	42.6	52.8	32.7
74.1	58.7	37.4	22.2	53.0	43.3	36.4	35.4	58.5	41.2		27.9	18.6	43.0	53.9	35.7
67.6	61.8	45.1	23.8	55.6	37.1	35.3	32.1	59.6	36.1		29.9	23.9	50.6	53.3	26.6
71.1	70.2	33.2	17.3	63.1	33.0	37.5	31.3	59.8	31.2		32.1	21.6	50.2	56.0	28.8
70.9	73.7	39.1	19.6	62.8	30.3	43.8	29.3	55.3	33.7		26.7	19.1	49.0	60.3	28.8
68.2	68.6	39.2	33.2	60.4	41.9	44.7	28.6	54.2	41.3		17.9	28.5	45.8	60.9	32.9
77.4	74.8	46.1	31.3	85.1	39.2	50.1	25.9	53.1	38.1		28.1	35.7	39.2	64.4	27.4
73.9	92.6	44.4	29.0	60.1	49.5	41.4	30.7	54.7	47.4		24.8	32.3	42.2	67.0	29.7
69.6	89.2	42.3	29.3	52.2	46.6	43.6	34.4	58.0	49.5		22.7	36.1	42.3	63.0	25.4
83.1	84.3	43.6	27.2	47.4	51.3	42.1	37.7	59.9	48.9		27.8	32.7	42.6	65.5	35.4
62.2	68.0	27.2	14.0	33.7	39.0	36.0	32.9	63.2	47.5		29.7	27.2	43.4	62.8	29.3
73.9	78.8	47.3	16.7	55.5	18.1	47.5	22.1	60.0	50.3		33.7	28.7	42.7	49.2	35.4
71.2	73.8	41.9	9.2	63.9	26.1	48.9	21.7	57.8	47.8		23.7	19.0	42.4	50.1	38.4
70.0	55.2	45.3	18.3	59.7	45.0	49.6	21.1	53.8	45.0		28.1	25.8	47.4	63.9	40.1
82.0	59.4	47.1	20.9	56.4	44.0	47.5	23.1	52.7	49.5		33.0	20.1	44.1	68.7	37.2
71.3	55.4	48.6	21.6	66.1	59.5	41.9	22.5	53.7	42.8		22.4	28.4	43.6	59.0	39.9
63.3	60.5	57.0	10.4	51.5	59.6	43.8	24.5	53.1	46.3		26.2	35.1	43.3	66.3	35.9
66.2	61.9	53.7	28.8	61.5	56.8	40.0	15.7	52.7	42.0		24.0	32.4	44.2	63.9	44.9
71.1	52.9	42.8	28.9	46.0	41.2	44.7	12.8	51.3	35.6		21.1	31.2	45.2	50.8	46.5
61.3	63.6	43.2	31.4	38.8	42.1	55.8	10.1	57.7	55.3		18.2	29.9	41.9	52.4	29.1
63.9	61.8	34.8	20.0	35.0	36.6	53.3	12.2	49.2	60.1		16.8	27.7	48.2	57.4	35.6
72.7	49.7	33.8	16.8	41.1	27.8	43.4	15.7	46.6	59.2		21.3	28.9	45.3	65.2	45.9
70.2	56.5	36.8	12.6	39.5	42.4	44.6	25.1	54.4	51.9		16.7	31.1	53.9	57.7	45.9
52.7	50.1	37.0	41.0	48.8	43.5	45.6	21.5	54.1	46.0		18.1	33.0	51.7	65.1	28.6
57.9	45.5	32.3	25.4	44.6	39.5	43.9	24.2	51.0	47.8		18.5	31.3	52.8	65.7	42.3
58.6	47.1	37.7	20.1	38.4	48.1	41.2	21.1	55.4	42.4		22.6	35.1	50.6	56.3	20.6
49.9	50.3	53.5	4.4	42.6	56.5	28.8	16.5	54.3	32.2		21.1	31.0	54.3	60.2	37.5
36.8	47.7	49.1	24.5	60.9	81.5	40.8	28.6	59.7	37.0		22.8	35.6	52.2	47.9	42.8
50.1	52.7	36.4	34.6	57.9		43.3	37.2	60.9	42.7		21.6	33.6	59.7	40.1	39.6
61.9	52.1	45.5	33.3	52.8		41.5	31.2	66.7	52.1		26.5	34.7	54.3	44.8	35.1
61.4	51.9	46.1	11.6	57.3		41.8	23.9	66.3	45.6		26.9	38.8	56.6	41.4	34.8
66.6	52.6	40.8	16.7	50.5		37.7	26.8	63.6	41.2		34.5	35.8	48.5	25.0	41.6
67.9	54.6	46.2	48.6	75.0		41.8	28.6	67.5	47.4		33.0	40.8	51.0	47.9	25.4
70.6	52.1	44.9	34.1	78.4		53.3	31.2	64.3	40.9		26.9	36.0	55.2	64.8	36.2
69.5	47.7	46.3	44.0	69.2		38.6	36.8	57.0	44.6		26.9	33.3	59.4	54.6	37.0
73.5	44.9	46.4	20.4	83.2		54.7	32.2	60.1	47.2		27.8	17.1	57.2	61.1	39.0
69.6	48.6	37.2	21.6	86.6		42.0	27.0	60.1	53.2		31.8	32.3	66.3	56.5	45.7
58.9	50.5	38.1	33.5	97.5		47.0	22.2	70.0	23.9		25.1	30.1	60.2	55.2	34.9
57.5	46.3	40.0	15.1	73.0		47.1	30.5	22.5	57.7		23.6	31.0	54.2	46.0	51.9
49.5	47.4	42.6	44.6	62.4		60.5	31.6	65.4	40.7		23.0	28.1	62.1	58.8	51.9
50.1	48.2	34.0	60.7	52.7		54.9	27.7	65.7	45.7		27.3	32.1	55.1	63.1	49.7
54.1	44.4	38.3	38.1	51.9		65.4	23.6	64.8	45.7		28.8	38.2	58.5	59.9	46.6
64.6	53.8	43.3	26.6	42.6		57.1	21.2	63.6	43.3		31.3	35.7	57.8	38.0	48.2
58.6	44.5	38.0	40.4	42.5		64.8	30.6	61.9	42.3		31.9	38.7	59.7	81.5	45.8
54.7	52.0	25.6	38.3	32.9		63.8	36.0	60.1	51.7		27.2	39.7	51.8	55.9	47.8
68.5	58.6	51.4	24.8	57.4		64.3	31.8	54.9	54.5		24.2	38.5	62.1	54.9	44.7
69.8	53.7	40.2	27.4	54.5		65.3	31.9	57.4	55.1		24.5	38.2	60.1	47.5	51.8
62.4	55.3	34.1	45.2	50.2		64.5	16.2	60.4	45.0		21.3	34.7	55.4	42.7	51.0
67.8	62.8	33.9	52.4	63.3		59.1	35.0	63.6	48.0		19.0	26.0	54.8	50.0	43.4
68.9	64.7	37.5	44.9	57.8		67.6	30.1	64.6	57.7		20.8	47.9	58.3	51.4	45.4
76.4	62.5	40.3	43.4	57.3		55.5	38.7	65.0	46.9		17.1	41.6	52.3	43.8	45.1
68.3	54.8	42.2	32.7	47.2		68.1	34.1	59.3	43.3		26.6	41.1	50.9	37.1	36.4
74.7	64.4	41.4	25.8	49.9		61.9	39.2	58.1	45.4		35.7	42.2	56.2	7.6	42.8
74.7	58.6	30.8	26.4	38.5		62.4	40.8	56.5	46.3		21.9	38.8	55.3	10.5	27.1
71.5	54.1	37.6	27.8	75.7		66.4	50.2	55.2	57.7		31.6	21.3	56.3	15.6	14.6
58.0	63.7	44.1	29.9	37.2		65.4	47.7	64.7	58.4		26.6	43.4	55.1	18.7	38.5
63.0	44.1	51.6	26.1	58.6		54.9	38.1	63.7	40.7		30.8	44.4	54.9	16.8	31.0
61.3	50.3	29.5	43.7	68.8		64.5	38.4	68.7	47.1		29.1	42.2	50.9	26.0	29.0
70.3	60.1	34.5	20.1	60.8		62.4	38.4	67.6	47.8		35.4	41.6	64.9	23.7	21.8
69.5	53.5	22.4	8.9	53.0		71.5	38.7	60.1	46.5		42.5	45.2	59.8	16.7	
73.9	35.3	35.5	15.6	54.7		73.5	40.7	53.2	44.6		36.6	46.4	52.4	20.9	
78.6	30.2	33.3	28.8	57.4		61.2	51.0	60.6	48.9		28.7	46.8	60.6	25.6	

## Appendix C: Soot Measurements

Site	Latitude	Longitude	mg C/cm <sup>2</sup> from visual comparison with standards	ng C/g from visual comparison with standard filters	Comments
Yukon River	66.25552	144.76890	0.0020	17.55	surface
			0.0025	12.60	0-20 cm depth
Porcupine River	67.56833	138.28667	0.0005	4.01	surface
			0.0014	9.28	0-20 cm depth
Mackenzie River	67.16000	130.25667	0.0005	3.69	surface
			0.0085	44.78	0-20 cm depth
Small Lake near Deline	64.93390	124.77438	0.0010	7.07	surface
			0.0012	12.99	0-20 cm depth
Great Bear Lake 1 (GB-1)	65.37922	122.66280	0.0009	5.78	surface
			0.0006	3.89	0-20 cm depth
Great Bear Lake 2	65.60676	122.26140	0.0006	4.88	surface
			0.0005	3.48	0-20 cm depth
Great Bear Lake 3	65.78752	121.78390	0.0009	6.44	surface
			0.0009	6.81	0-20 cm depth
Great Bear Lake 4	66.22479	121.06220	0.0006	6.34	surface
			0.0009	6.86	0-20 cm depth
Great Bear Lake 5	66.35284	120.63710	0.0007	6.55	surface
			0.0008	6.85	0-20 cm depth
Dease River	66.90020	118.93787	0.0020	19.35	surface
			0.0010	6.04	0-20 cm depth
Bloody Falls	67.74865	115.37532	0.0030	37.06	surface (dirt?)
			0.0120	103.57	0-20 cm depth (dirt)
KD3	66.65447	113.55992	0.0030	23.13	surface
			0.0007	5.25	0-20 cm depth
Rockinghorse Lake	65.95683	112.42167	0.0004	4.07	surface
			0.0013	7.60	0-20 cm depth
Yamba Lake	65.08667	111.45447	0.0007	7.42	surface
			0.0010	9.25	0-20 cm depth
Lake Providence	64.74738	111.85403	0.0013	14.85	surface
			0.0012	9.17	0-20 cm depth
Diavik (DB-1)	64.58344	110.75402	0.0030	27.17	surface
			0.0030	19.57	0-20 cm depth

Lac De Gras	64.52760	110.53655	0.0040	41.38	surface
			0.0010	8.84	0-20 cm depth
Thonokied Lake	64.35160	109.68070	0.0012	9.42	surface
			0.0010	8.32	0-20 cm depth
Alymer Lake	64.08630	108.50971	0.0020	19.35	surface
			0.0022	16.07	0-20 cm depth
Clinton-Colden Lake	64.01122	107.57671	0.0009	10.18	surface
			0.0012	8.44	0-20 cm depth
Sifton Lake	63.75079	106.54487	0.0005	4.10	surface
			0.0010	6.12	0-20 cm depth
Hoare Lake	63.61069	105.12755	0.0010	11.22	surface
			0.0012	9.31	0-20 cm depth
Hornby Point	64.03854	103.85468	0.0010	7.25	surface
			0.0008	6.06	0-20 cm depth
Thelon Lookout Point	64.17569	102.50803	0.0015	11.93	surface
			0.0020	11.16	0-20 cm depth
Thelon Cabin	64.53258	101.35525	0.0005	4.33	surface
			0.0010	5.74	0-20 cm depth
Beverly Lake	64.62036	100.47297	0.0005	3.40	surface
			0.0005	4.04	0-20 cm depth
Aberdeen Lake	64.57758	98.54950	0.0004	3.77	surface
			0.0004	3.52	0-20 cm depth
Baker	64.41800	96.40628	0.0008	7.43	surface
			0.0007	4.46	0-20 cm depth

## Appendix D: Mercury Measurements

Site	Latitude	Longitude	From visual comparison with standards		Depth	Hg sample name	Hg sample name on tape	Hg conc (pg/g)	Notes	Collection time
			(mgC/cm <sup>2</sup> )	(ngC/g)						
Yukon River	66.25552	144.76890	0.00200	17.54959	surface	25W35	07-28	10.70	top 2-3 cm	
			0.00250	12.59748	0-20 cm	25W43	07-27	2.32		
Porcupine River	67.56833	138.28667	0.00050	4.01371	surface	25W17	07-105	6.90	surface	17:53
			0.00140	9.27752	0-20 cm	G222	07-110	7.12		
Mackenzie River	67.16000	130.25667	0.00050	3.68796	surface	G58	07-66	11.35		9:40
			0.00850	44.78233	0-20 cm	G100	07-65	5.34		
Small Lake near Deline	64.93390	124.77438	0.00100	7.06858	surface	G30	07-62	23.07		15:50
			0.00120	12.99416	0-20 cm	G43	07-102	8.55		
Great Bear Lake 1 (GB-1)	65.37922	122.66280	0.00090	5.78339	surface	CRREL-103	07-44	5.30		16:30
			0.00060	3.88502	0-20 cm	25W13	07-43	4.99		
Great Bear Lake 2	65.60676	122.26140	0.00060	4.87800	surface	G82	07-52	3.98		10:00
			0.00050	3.47635	0-20 cm	-	07-2	4.34		
Great Bear Lake 3	65.78752	121.78390	0.00085	6.43746	surface	G11	07-34	9.85		13:30
			0.00090	6.81309	0-20 cm	G50	07-32	5.35		
Great Bear Lake 4	66.22479	121.06220	0.00060	6.33533	surface	CRREL-118	07-16	8.00		11:15
			0.00090	6.85695	0-20 cm	25W49	07-17	2.89		
Great Bear Lake 5	66.35284	120.63710	0.00070	6.54883	surface	G218	07-20	6.97		14:00
			0.00080	6.85438	0-20 cm	25W50?	07-18	1.57		
Dease River	66.90020	118.93787	0.00200	19.35126	surface	G210	07-108	26.68		10:10
			0.00100	6.04439	0-20 cm	25W51	07-15	6.00		
Bloody Falls	67.74865	115.37532	0.00300	37.05859	surface (dirt?)	25W56	07-19	32.04	all new snow from last night	11:10
			0.01200	103.56899	0-20 cm (dirt)	25W37	07-21	2.35		

KD3	66.65447	113.55992	0.00300	23.13355	surface	G40	07-63	3.77		15:00
			0.00070	5.25452	0-20 cm	G5	07-69	2.90		
Rockinghorse Lake	65.95683	112.42167	0.00036	4.07150	surface	G41	07-48	4.29	all new surface snow: 1 day overnight	12:45
			0.00130	7.60482	0-20 cm	G74	07-58	1.72		
Yamba Lake	65.08667	111.45447	0.00070	7.42201	surface	G14	07-36	4.91		12:30
			0.00100	9.25342	0-20 cm	G26	07-37	3.14		
Lake Providence	64.74738	111.85403	0.00130	14.85117	surface	CRREL 100?	07-107	4.41		16:00
			0.00120	9.17005	0-20 cm	G227?	07-106	6.59		
Diavik (DB-1)	64.58344	110.75402	0.00300	27.16751	surface	25W12	07-82	5.43		13:00
			0.00300	19.57454	0-20 cm	G215	07-83	2.00		
Lac De Gras	64.52760	110.53655	0.00400	41.37707	surface	G9	07-40	30.55		14:00
			0.00100	8.83573	0-20 cm	G27	07-41	5.65		
Thonokied Lake	64.35160	109.68070	0.00120	9.42478	surface	G216	07-81	3.07		14:00
			0.00100	8.31598	0-20 cm	25W34	07-30	1.34		
Alymer Lake	64.08630	108.50971	0.00200	19.35126	surface	CRREL-136	07-79	2.06		18:30
			0.00220	16.07326	0-20 cm	-	07-100	1.02		
Clinton-Colden Lake	64.01122	107.57671	0.00090	10.17876	surface	G53	07-9	3.27		13:30
			0.00120	8.43544	0-20 cm	G88	07-8	2.27		
Sifton Lake	63.75079	106.54487	0.00050	4.10434	surface	G225	07-115	6.09		10:00
			0.00100	6.11704	0-20 cm	G220	07-114	6.90		
Hoare Lake	63.61069	105.12755	0.00100	11.21997	surface	G33	07-70	7.24	snowing lightly; new and recent	10:30
			0.00120	9.30842	0-20 cm	G70	07-67	1.76		
Hornby Point	64.03854	103.85468	0.00100	7.24983	surface	G72	07-38	7.47		10:00
			0.00080	6.05608	0-20 cm	G98	07-39	1.89		
Thelon Lookout Point	64.17569	102.50803	0.00150	11.92823	surface	G23	07-104	9.40		11:00
			0.00200	11.16092	0-20 cm	CRREL-128	07-103	1.91		



Thelon Cabin	64.53258	101.35525	0.00050	4.32770	surface	G80	07-10	11.51		17:00
			0.00100	5.74422	0-20 cm	G96	07-61	2.10		
Beverly Lake	64.62036	100.47297	0.00050	3.40199	surface	G214	07-99	4.00		11:00
			0.00050	4.03919	0-20 cm	25W33	07-31	BD		
Aberdeen Lake	64.57758	98.54950	0.00040	3.76991	surface	G61	07-49	3.94		11:00
			0.00040	3.52206	0-20 cm	G13	07-50	2.29		
Baker	64.41800	96.40628	0.00080	7.42975	surface	G206	07-80	7.91		13:00
			0.00072	4.45785	0-20 cm	CRREL-115	07-101	2.10		

## Appendix E: Ion Measurements

Site	Latitude	Longitude	Depth	From visual comparison with standards		IC Name	S cond (µS)	Chloride (µM)	Bromide (µM)	Nitrate (µM)	Sulfate (µM)	Sodium (µM)	Ammonium (µM)	Potassium (µM)	Magnesium (µM)	Calcium (µM)
				(mgC/cm <sup>2</sup> )	(ngC/g)											
Yukon River	66.25552	144.76890	surface	0.00200	17.54959	S 40	4.4	6.2299	0.0671	3.2058	4.0692	3.0342	3.8527	1.5172	2.0373	7.4249
			0-20 cm	0.00250	12.59748	V 40	4.41	1.985	0.019	2.261	1.279	1.233	0.3897	0.5011	0.786	3.2743
Porcupine River	67.56833	138.28667	surface	0.00050	4.01371	S 18	3.56	0.703	0.026	1.434	0.663	0.4667	0.4804	0.0619	0.1635	0.6741
			0-20 cm	0.00140	9.27752	V 18										
Mackenzie River	67.16000	130.25667	surface	0.00050	3.68796	S 44	5.04	6.187	0.041	2.727	2.364	1.3471	0.7467	0.1184	0.4343	1.5422
			0-20 cm	0.00850	44.78233	V 44	4.06	2.221	0.019	1.814	0.659	0.8084	0.7355	0.054	0.4674	1.2824
Small Lake near Deline	64.93390	124.77438	surface	0.00100	7.06858	S 09	7.38	5.851	0.082	2.983	1.988	1.7388	0.7023	0.2467	1.1326	2.1555
			0-20 cm	0.00120	12.99416	V 09	3.97	1.789	0.021	2.739	2.031	0.7589	0.5416	0.1095	1.3405	2.6104
Great Bear Lake 1 (GB-1)	65.37922	122.66280	surface	0.00090	5.78339	S 48	5.94	2.518	0.059	1.998	1.819	1.4756	0.4409	0.0722	0.5399	1.0553
			0-20 cm	0.00060	3.88502	V 48	5.09	2.536	0.010	3.649	0.997	1.5043	0.7076	0.0656	0.8907	1.6214
Great Bear Lake 2	65.60676	122.26140	surface	0.00060	4.87800	S 24	3.91	4.011	0.035	1.650	1.972	2.8181	1.3236	0.1171	0.6169	0.7779
			0-20 cm	0.00050	3.47635	V 24										
Great Bear Lake 3	65.78752	121.78390	surface	0.00085	6.43746	S 02	8.24	4.792	0.083	3.592	2.267	2.4545	0.5928	0.1086	0.6812	1.0313
			0-20 cm	0.00090	6.81309	V 02	6.14	4.502	0.041	2.915	2.075	2.7632	0.5343	0.1494	1.4412	1.8724
Great Bear Lake 4	66.22479	121.06220	surface	0.00060	6.33533	S 30	11.64	10.151	0.099	2.690		2.7822	1.0249	0.1437	0.8769	1.4553
			0-20 cm	0.00090	6.85695	V 30										
Great Bear Lake 5	66.35284	120.63710	surface	0.00070	6.54883	S 32	8.36	8.503	0.090	4.598	4.185	4.593	0.9983	0.3928	1.6117	1.243
			0-20 cm	0.00080	6.85438	V 32										
Dease River	66.90020	118.93787	surface	0.00200	19.35126	S 36										
			0-20 cm	0.00100	6.04439	V 36	4.83	3.621	0.033	3.872	1.576	1.9472	0.6492	0.1262	0.4816	1.1734

Bloody Falls	67.74865	115.37532	surface (dirt?)	0.00300	37.05859	S 17	11.66	9.280	0.154	20.111	11.388	6.3548	9.4557	0.8347	4.4286	9.2302
			0-20 cm (dirt)	0.01200	103.56899	V 17										
KD3	66.65447	113.55992	surface	0.00300	23.13355	S 04	8.16	5.738	0.113	10.740	7.786	3.8647	5.3958	0.299	2.5876	5.4442
			0-20 cm	0.00070	5.25452	V 04	5.35	5.649	0.055	5.373	2.968	2.9419	1.7012	0.2352	1.0537	1.2598
Rockinghorse Lake	65.95683	112.42167	surface	0.00036	4.07150	S 19	9.98	1.072	0.011	11.298	1.583	0.3886	2.596	0.0546	0.5412	2.2
			0-20 cm	0.00130	7.60482	V 19	10.23	3.134	0.021	6.951	2.359	1.7612	0.6559	0.1216	0.4786	0.8357
Lake Providence	64.74738	111.85403	surface	0.00130	14.85117	S 13	8.76	0.992	0.049	6.405	4.412	0.7471	4.6318	0.1764	0.6678	1.0158
			0-20 cm	0.00120	9.17005	V 13	9.37	4.243	0.043	8.244	2.883	1.9404	2.1344	0.1381	0.8125	0.957
Yamba Lake	65.08667	111.45447	surface	0.00070	7.42201	S 01	7.38	0.791	0.019	6.187	2.824					
			0-20 cm	0.00100	9.25342	V 01	7.19	3.996	0.030	5.201	3.075	2.364	1.1829	0.1378	0.8496	0.8785
Diavik (DB-1)	64.58344	110.75402	surface	0.00300	27.16751	S 26	6.91	1.4633	0.0687	11.2045	7.8117	1.1574	6.0205	0.4598	1.7084	2.5479
			0-20 cm	0.00300	19.57454	V 26	6.82	6.618	0.060	5.273	4.441	3.5594	0.8874	10.6649	2.9673	23.3018
Lac De Gras	64.52760	110.53655	surface	0.00400	41.37707	S 42	7.25	2.000	0.073	8.510	6.521	1.4562	6.5668	1.3398	3.4266	3.9442
			0-20 cm	0.00100	8.83573	V 42	7.11	3.000	0.038	7.136	3.527	1.5287	2.3044	0.3638	1.766	1.7678
Thonokied Lake	64.35160	109.68070	surface	0.00120	9.42478	S 15	8.9	1.837	0.036	7.085	4.688	1.1382	4.8578	0.1132	0.6709	1.2846
			0-20 cm	0.00100	8.31598	V 15	12.18	1.504	0.018	4.767	2.757	1.2077	2.2048	0.2372	0.5916	1.2022
Alymer Lake	64.08630	108.50971	surface	0.00200	19.35126	S 22	9.36	4.397	0.050	8.574	10.381	1.2932	8.0554	0.265	1.0363	2.5682
			0-20 cm	0.00220	16.07326	V 22	7.93	3.550	0.043	5.844	3.985	1.7529	2.1725	0.1412	0.6649	1.732
Clinton-Colden Lake	64.01122	107.57671	surface	0.00090	10.17876	S 49	8.29	2.218	0.095	6.157	5.834	1.7325	4.45	0.1261	0.7215	1.4622
			0-20 cm	0.00120	8.43544	V 49	8.05	16.0627	0.0316	8.4294	5.6372	8.6827	2.985	0.4954	1.8788	2.1182
Sifton Lake	63.75079	106.54487	surface	0.00050	4.10434	S 33	5.43	2.015	0.037	3.671	1.882	1.5373	1.3974	0.1782	0.5633	1.0392
			0-20 cm	0.00100	6.11704	V 33	5.94	4.845	0.041	5.194	3.157	3.1065	1.2436	0.1823	0.8609	1.0521
Hoare Lake	63.61069	105.12755	surface	0.00100	11.21997	S 46	8.04	2.9885	0.0505	6.4819	5.6605	1.8514	3.8621	0.5824	0.9722	1.9471
			0-20 cm	0.00120	9.30842	V 46	6.02	5.682	0.032	5.904	1.823	2.8906	0.9042	0.1209	0.6117	0.8269
Hornby Point	64.03854	103.85468	surface	0.00100	7.24983	S 43	10.06	3.373	0.064	5.991	4.144	2.1128	2.4159	0.1111	0.6122	1.0547
			0-20 cm	0.00080	6.05608	V 43										

Thelon Lookout Point	64.17569	102.50803	surface	0.00150	11.92823	S 31	10.38	6.5061	0.1716	10.4943	7.0638	2.9642	2.6739	0.2559	1.0622	2.0695
			0-20 cm	0.00200	11.16092	V 31	10.5	6.921	0.047	10.991	3.197	3.5536	1.7366	0.2701	0.9212	1.1588
Thelon Cabin	64.53258	101.35525	surface	0.00050	4.32770	S 11	5.07	2.344	0.041	2.998	1.529	1.8126	1.4166	0.115	0.4557	0.7797
			0-20 cm	0.00100	5.74422	V 11	7.82	10.733	0.030	3.894	2.619	6.8053	1.371	0.4999	1.9161	1.3921
Beverly Lake	64.62036	100.47297	surface	0.00050	3.40199	S 14	9.18	9.256	0.072	7.628	3.698	4.8728	2.3825	0.1861	1.0144	0.9749
			0-20 cm	0.00050	4.03919	V 14	6.55	11.297	0.062	5.313	2.764	7.7667	1.819	0.3058	1.6805	1.2641
Aberdeen Lake	64.57758	98.54950	surface	0.00040	3.76991	S 50	7.48	2.478	0.033	2.842	1.619	1.2717	1.9798	0.0547	0.2864	0.7604
			0-20 cm	0.00040	3.52206	V 50	8	3.658	0.059	6.201	2.558	2.2895	3.1973	0.1265	0.558	0.9445
Baker	64.41800	96.40628	surface	0.00080	7.42975	S 29	5.48	2.491	0.046	3.156	2.209	1.5987	2.8999	0.0855	0.3995	0.8056
			0-20 cm	0.00072	4.45785	V 29	5.69	3.228	0.070	6.509	3.499	2.0106	4.7294	0.1535	0.8198	1.5877

## Appendix F: Isotope Measurements

Site Name	Latitude	Longitude	Pit Interval	Sample designator	$\delta^{18}\text{O}$	$\delta\text{D}$ (‰)		
					Average	Standard dev.	Average	Standard dev.
Yukon River	66.25552	144.76890	surface	S 40	-36.7	0.1	-272.1	0.5
	66.25552	144.76890	0-20 cm	V 40	-32.7	0.1	-241.5	0.7
Porcupine River	67.56833	138.28667	surface	S 18	-34.9	0.1	-266.5	0.3
	67.56833	138.28667	0-20 cm	V 18	-32.2	0.1	-243.7	0.7
Mackenzie River	67.16000	130.25667	surface	S 44	-28.7	0.0	-213.9	0.6
	67.16000	130.25667	0-20 cm	V 44				
Small Lake near Deline	64.93390	124.77438	surface	S 09	-26.8	0.0	-205.7	0.6
	64.93390	124.77438	0-20 cm	V 09				
Great Bear Lake 1 (GB-1)	65.37922	122.66280	surface	S 48	-28.3	1.2	-214.0	0.6
	65.37922	122.66280	0-20 cm	V 48	-28.8	0.1	-219.2	0.3
Great Bear Lake 2	65.60676	122.26140	surface	S 24	-28.0	0.0	-212.3	0.7
	65.60676	122.26140	0-20 cm	V 24				
Great Bear Lake 3	65.78752	121.78390	surface	S 02				
	65.78752	121.78390	0-20 cm	V 02	-27.4	0.1	-209.6	0.8
Great Bear Lake 4	66.22479	121.06220	surface	S 30	-28.7	0.2	-222.5	1.4
	66.22479	121.06220	0-20 cm	V 30				
Great Bear Lake 5	66.35284	120.63710	surface	S 32	-29.7	0.1	-232.6	0.3
	66.35284	120.63710	0-20 cm	V 32				
Dease River	66.90020	118.93787	surface	S 36	-28.7	0.0	-229.1	0.2
	66.90020	118.93787	0-20 cm	V 36				
Bloody Falls	67.74865	115.37532	surface (dirt?)	S 17				
	67.74865	115.37532	0-20 cm (dirt)	V 17	-29.7	0.1	-226.3	0.8

KD3	66.65447	113.55992	surface	S 04	-26.3	0.1	-204.3	0.4
	66.65447	113.55992	0-20 cm	V 04	-31.1	0.1	-237.5	0.4
Rockinghorse Lake	65.95683	112.42167	surface	S 19	-26.2	0.4	-197.7	1.3
	65.95683	112.42167	0-20 cm	V 19	-25.9	0.1	-193.3	1.0
Lake Providence	64.74738	111.85403	surface	S 13	-23.5	0.0	-173.2	0.3
	64.74738	111.85403	0-20 cm	V 13	-28.9	0.1	-221.4	0.4
Yamba Lake	65.08667	111.45447	surface	S 01	-24.0	0.1	-187.8	0.8
	65.08667	111.45447	0-20 cm	V 01	-26.5	0.2	-202.4	1.0
Diavik (DB-1)	64.58344	110.75402	surface	S 26	-23.8	0.3	-177.8	1.0
	64.58344	110.75402	0-20 cm	V 26	-27.8	0.0	-207.6	0.5
Lac De Gras	64.52760	110.53655	surface	S 42	-24.2	0.1	-178.7	0.7
	64.52760	110.53655	0-20 cm	V 42	-30.7	0.0	-238.4	0.3
Thonokied Lake	64.35160	109.68070	surface	S 15				
	64.35160	109.68070	0-20 cm	V 15	-23.9	0.0	-179.1	0.6
Alymer Lake	64.08630	108.50971	surface	S 22	-19.2	0.1	-144.3	0.7
	64.08630	108.50971	0-20 cm	V 22	-30.1	0.0	-230.5	0.3
Clinton-Colden Lake	64.01122	107.57671	surface	S 49	-23.7	0.2	-180.9	1.6
	64.01122	107.57671	0-20 cm	V 49	-24.8	0.1	-186.3	0.2
Sifton Lake	63.75079	106.54487	surface	S 33	-27.1	0.1	-208.7	0.4
	63.75079	106.54487	0-20 cm	V 33	-29.1	0.0	-222.6	0.5
Hoare Lake	63.61069	105.12755	surface	S 46	-24.6	0.0	-182.1	0.2
	63.61069	105.12755	0-20 cm	V 46	-27.6	0.1	-208.9	0.1
Hornby Point	64.03854	103.85468	surface	S 43				
	64.03854	103.85468	0-20 cm	V 43	-27.8	0.0	-207.0	0.2
Thelon Lookout Point	64.17569	102.50803	surface	S 31				
	64.17569	102.50803	0-20 cm	V 31	-29.2	0.0	-220.8	0.5
Thelon Cabin	64.53258	101.35525	surface	S 11	-26.7	0.0	-198.0	0.6
	64.53258	101.35525	0-20 cm	V 11				
Beverly Lake	64.62036	100.47297	surface	S 14	-24.2	0.1	-186.6	0.6
	64.62036	100.47297	0-20 cm	V 14	-25.1	0.0	-190.5	0.4

Aberdeen Lake	64.57758	98.54950	surface	S 50	-24.7	0.1	-180.3	0.3
	64.57758	98.54950	0-20 cm	V 50	-25.4	0.0	-193.2	1.1
Baker	64.41800	96.40628	surface	S 29	-24.4	0.0	-179.5	0.2
	64.41800	96.40628	0-20 cm	V 29	-25.3	0.1	-188.1	0.7

# REPORT DOCUMENTATION PAGE

*Form Approved*  
OMB No. 0704-0188

Public reporting burden for this collection of information is estimated to average 1 hour per response, including the time for reviewing instructions, searching existing data sources, gathering and maintaining the data needed, and completing and reviewing this collection of information. Send comments regarding this burden estimate or any other aspect of this collection of information, including suggestions for reducing this burden to Department of Defense, Washington Headquarters Services, Directorate for Information Operations and Reports (0704-0188), 1215 Jefferson Davis Highway, Suite 1204, Arlington, VA 22202-4302. Respondents should be aware that notwithstanding any other provision of law, no person shall be subject to any penalty for failing to comply with a collection of information if it does not display a currently valid OMB control number. **PLEASE DO NOT RETURN YOUR FORM TO THE ABOVE ADDRESS.**

<b>1. REPORT DATE (DD-MM-YYYY)</b> February 2008		<b>2. REPORT TYPE</b> Technical Report		<b>3. DATES COVERED (From - To)</b>	
<b>4. TITLE AND SUBTITLE</b>  A Reconnaissance Snow Survey Across Northwest Territories and Nunavut, Canada, April 2007				<b>5a. CONTRACT NUMBER</b>	
				<b>5b. GRANT NUMBER</b>	
				<b>5c. PROGRAM ELEMENT NUMBER</b>	
<b>6. AUTHOR(S)</b>  Matthew Sturm, Chris Derksen, Glen Liston, Arvids Silis, Daniel Solie, Jon Holmgren, and Henry Huntington				<b>5d. PROJECT NUMBER</b>	
				<b>5e. TASK NUMBER</b>	
				<b>5f. WORK UNIT NUMBER</b>	
<b>7. PERFORMING ORGANIZATION NAME(S) AND ADDRESS(ES)</b>  U.S. Army Engineer Research and Development Center Cold Regions Research and Engineering Laboratory 72 Lyme Road Hanover, NH 03755-1290				<b>8. PERFORMING ORGANIZATION REPORT NUMBER</b>  ERDC/CRREL TR-08-3	
<b>9. SPONSORING / MONITORING AGENCY NAME(S) AND ADDRESS(ES)</b>  National Science Foundation  Environment Canada				<b>10. SPONSOR/MONITOR'S ACRONYM(S)</b>	
				<b>11. SPONSOR/MONITOR'S REPORT NUMBER(S)</b>	
<b>12. DISTRIBUTION / AVAILABILITY STATEMENT</b> Approved for public release; distribution is unlimited.  Available from NTIS, Springfield, Virginia 22161.					
<b>13. SUPPLEMENTARY NOTES</b>					
<b>14. ABSTRACT</b> During April 2007, a coordinated series of snow measurements were made across the Northwest Territories and Nunavut, Canada, during a 4200-km snowmobile traverse from Fairbanks, Alaska, to Baker Lake, Nunavut. While detailed, local snow measurements have been made as part of ongoing studies at tundra field sites in this region (Daring Lake and Trail Valley Creek in the Northwest Territories), systematic measurements at the regional scale have not been previously collected across this region. Consistent with observations of tundra snow in Alaska and northern Manitoba, the snow cover consisted of depth hoar and wind slab with small and ephemeral fractions of new, recent, and icy snow. The snow was shallow (<40 cm deep), usually with less than six layers. Where deposited on lake and river ice, the snow was shallower, denser, and more metamorphosed than where deposited on tundra. The snow characteristics were highly variable at a local scale, but no longitudinal gradients in snow distribution, magnitude, or structure were detected. Lakes and lake ice confounded passive microwave remote sensing of the snow cover in this area because the lake signal overwhelmed the snow signal. Consequently, challenges remain in developing methods to monitor this snow cover by satellite.					
<b>15. SUBJECT TERMS</b> Northwest Territories Nunavut			Snow Snow cover Snow measurements		
<b>16. SECURITY CLASSIFICATION OF:</b>			<b>17. LIMITATION OF ABSTRACT</b>	<b>18. NUMBER OF PAGES</b>	<b>19a. NAME OF RESPONSIBLE PERSON</b>
<b>a. REPORT</b>	<b>b. ABSTRACT</b>	<b>c. THIS PAGE</b>			<b>19b. TELEPHONE NUMBER (include area code)</b>
U	U	U	U	89	